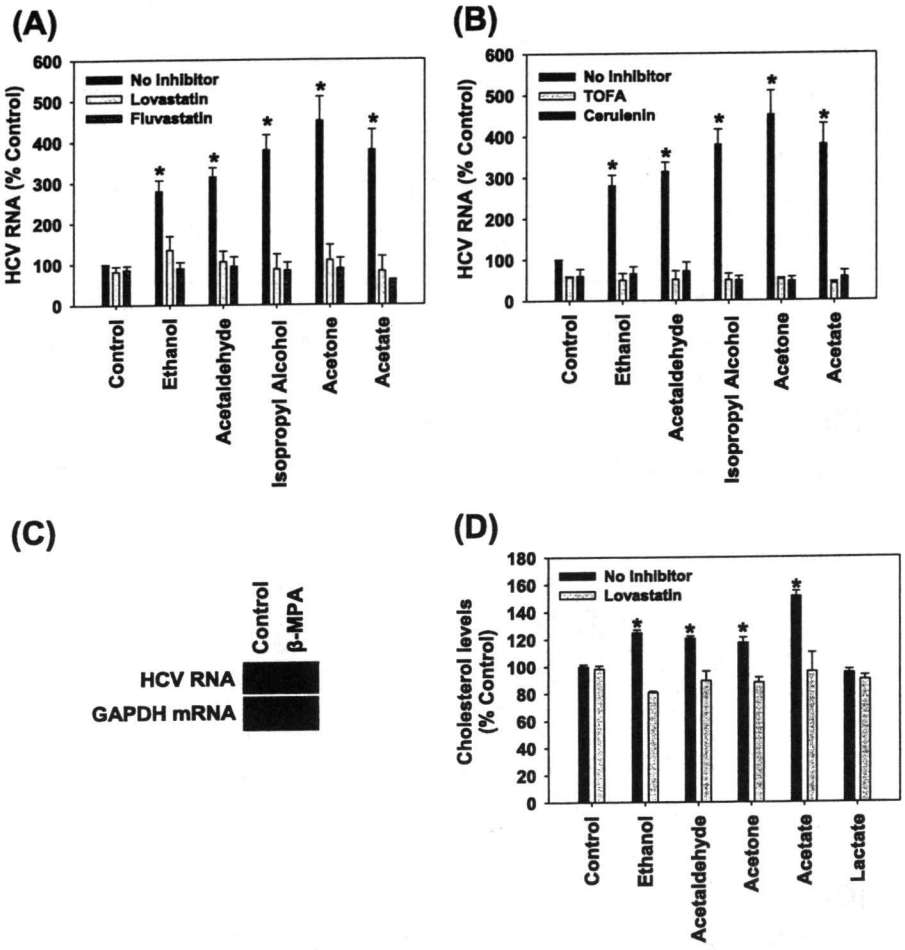

FIGURE 7. **Role of lipogenesis in the enhancement of HCV replication by ethanol, acetaldehyde, isopropyl alcohol, acetone, and acetate.** SgPC2 cells were treated for 24 h with (*A* and *B*) 0.2% ethanol, 5 μM acetaldehyde, 0.2% isopropyl alcohol, 2 mM acetone, 5 μM acetate ± 30 min pretreatment with (*A*) 5 μM lovastatin, 5 μM fluvastatin, (*B*) 5 μg/ml TOFA, 5 μg/ml cerulenin, or with (*C*) 2 mM β-mercaptopropionic acid (β-MPA). Then, HCV RNA levels were monitored by Northern blot and quantified by densitometry ($n = 3$). *D*, SgPC2 cells, treated for 24 h with ethanol, acetaldehyde, acetone, and acetate ± lovastatin, were monitored for cholesterol levels ($n = 3$). Lovastatin was activated, as described, before use (29). *, indicates statistically significant difference for indicated sample sizes ($p < 0.05$).

statin (Fig. 7*D*). Regarding potential effects of NADH on the ATP, overall ATP levels were not significantly perturbed in these cells by ethanol or other treatments (data not shown), suggesting that ATP is not likely to explain the effects that ethanol had on HCV. In fact, ethanol also increased the rate of HCV replication in the *in vitro* replication assay (Fig. 2*C* and 2*D*) which was performed in the presence of excess ATP. Taken together, these data indicate that the potentiation of HCV replication by ethanol, acetaldehyde, acetate, isopropyl alcohol, and acetone ultimately requires host lipid metabolism and is sensitive to lipid modulators, which points to potential targets for therapy. The concentrations of lovastatin and fluvastatin used here are higher than the doses used clinically to treat hypercholesterolemia. However, it is possible that statins, if used in combination with antivirals or other lipid modulators, will help control HCV replication, particularly in chronic alcoholics who show resistance to standard anti-HCV therapy (35). It is also interesting to note that the concentrations of acetone that enhanced HCV replication in this study are physiological levels that can be attained during metabolic dysfunction such as diabetes and during starvation (27), and HCV infection can lead to insulin resistance (36). In addition, acetate, which increased HCV replication at μM to mM concentrations in this study (Fig. 6*B* and data not shown), is used in hemodialysis.

Interestingly, increasing the NADH/NAD^+ ratio with lactate was not sufficient to increase HCV replication, suggesting that other factors may also play a role (Fig. 7*D*). Lactate also did not increase the intracellular cholesterol level. These results are consistent with an important role of cholesterol in the regulation of HCV replication. The data also indicate that even though ethanol and lactate both increase the NADH/NAD^+ ratio, ethanol is more lipogenic than lactate in these cells. The reason for these differences is unclear but it might be explained at least in part by the fact that ethanol can inhibit citric acid cycle as well as gluconeogenesis, which may cause acetate/acetyl-CoA produced by ethanol metabolism to be shunted more toward the lipogenic pathways, whereas these processes are likely to be stimulated by lactate (37). Ethanol can also decrease the total oxidation of fatty acids to CO_2, and increase the breakdown of glycogen, which may further drive lipogenesis in these cells (37–39). Further investigation into these effects will be beneficial to understanding how different metabolic conditions would affect HCV replication in hepatocytes.

Recently, McCartney *et al.* (7) reported an elevation of HCV RNA by ethanol in Huh7 replicon cells, transfected with

FIGURE 6. **Role of NADH/NAD^+ in the potentiation of HCV replication by ethanol, acetaldehyde, acetate, isopropyl alcohol, and acetone.** SgPC2 cells, supporting Con1 subgenomic HCV RNA replication, were treated with (*A*) 0.2% ethanol ± 0.1 mM 4MP plus 25 μM DADS or 0.1 mM cyanamide ($n = 3$); (*B*) 0.2% ethanol, 5 μM acetaldehyde, 5 μM acetate, 0.2% isopropyl alcohol, 2 mM acetone, or 25 mM *tert*-butanol ($n = 4$); (*C*) 0.2% ethanol, 5 μM acetaldehyde, 5 μM acetate, 0.2% isopropyl alcohol, and 2 mM acetone, with and without 5 mM pyruvate ($n = 3$); or (*D*) 0.2% ethanol or 5 mM lactate for 3 h for NADH/NAD^+ ratio measurement or 24 h for HCV RNA levels. HCV RNA levels were monitored by Northern blot (*A–D, left panels*). NADH/NAD^+ ratios were measured by an enzymatic NADH recycling assay, as described under "Experimental Procedures" (*A–D, right panels*). Northern blots were quantified by densitometry. *, indicates statistically significant difference for indicated sample sizes ($p < 0.05$).

CYP2E1; the effect could be suppressed by NAC, leading to the conclusion that the increase was due to ROS generation by CYP2E1. In contrast, we have consistently found that ROS suppresses HCV replication whereas antioxidants tend to counter this suppression (10–14) (Fig. 4). In particular, our BSO studies clearly demonstrate that endogenous ROS are sufficient to suppress HCV replication in cell culture (10, 11). Also, NAC and vitamin E either enhanced or had no significant effect on the potentiation of HCV replication by ethanol (Fig. 4*G*) as well as acetaldehyde, isopropyl alcohol, acetone, and acetate (data not shown). The reason for this discrepancy is unclear. However, CYP2E1 generates acetaldehyde as well as ROS, both of which can react with thiols, such as cysteine and GSH, which are generated from NAC, and the study by McCartney *et al.* did not differentiate whether the potentiation of HCV replication by ethanol was due to ROS, acetaldehyde, or other variables (7, 28). NAC can also have other effects on cells, including alteration of the pH and acting as a pro-oxidant, and careful monitoring of the pH and comparison with other antioxidants and pro-oxidants, therefore, are necessary. Indeed, our findings have been recently corroborated by other studies that show that HCV RNA replication is enhanced by antioxidants (*e.g.* vitamins E and C) and suppressed by lipid peroxidation products and ROS (12–14, 40). The mechanism by which ROS suppresses HCV replication is still not completely clear but it is likely to involve calcium and the dissociation of HCV replication complex from the membranes (10, 11). Detailed understanding of the mechanism by which ROS suppresses HCV replication and how acetaldehyde, NADH, acetyl-CoA, and ROS affect HCV *in vivo* will require additional *in vitro* and animal studies.

Therefore, we show that physiological levels of ethanol, acetaldehyde, and acetone promote HCV replication in the context of the complete HCV replication, and that the response is likely mediated by the modulation of host lipid metabolism requiring elevated NADH/NAD^+. Further study into the precise mechanisms of this regulation may lead to the development of novel treatments that target both the virus and its pathogenic interactions with ethanol in chronic hepatitis C patients.

Acknowledgments—We thank Anna Nandipati and Albert Sun for technical assistance. We also thank Dr. Jerome Lasker for CYP2E1 antibodies, Dr. Stanley Lemon for pRL-HL construct, and Dr. Charles Rice/Apath, LLC for Clone B and Huh7.5 cells. We also thank Drs. Arthur Cederbaum and T. S. Benedict Yen for discussion.

REFERENCES

1. Jamal, M. M., and Morgan, T. R. (2003) *Best Pract. Res. Clin. Gastroenterol.* **17,** 649–662
2. Sata, M., Fukuizumi, K., Uchimura, Y., Nakano, H., Ishii, K., Kumashiro, R., Mizokami, M., Lau, J. Y., and Tanikawa, K. (1996) *J. Viral. Hepat.* **3,** 143–148
3. Zhang, T., Li, Y., Lai, J. P., Douglas, S. D., Metzger, D. S., O'Brien, C. P., and Ho, W. Z. (2003) *Hepatology* **38,** 57–65
4. Seronello, S., Sheikh, M. Y., and Choi, J. (2007) *Free Radic. Biol. Med.* **43,** 869–882
5. Cromie, S. L., Jenkins, P. J., Bowden, D. S., and Dudley, F. J. (1996) *J. Hepatol.* **25,** 821–826
6. Tamai, T., Seki, T., Shiro, T., Nakagawa, T., Wakabayashi, M., Imamura, M., Nishimura, A., Yamashiki, N., Takasu, M., Inoue, K., and Okamura, A. (2000) *Alcohol Clin. Exp. Res.* **24,** Suppl. 4, 106S–111S
7. McCartney, E. M., Semendric, L., Helbig, K. J., Hinze, S., Jones, B., Weinman, S. A., and Beard, M. R. (2008) *J. Infect. Dis.* **198,** 1766–1775
8. Trujillo-Murillo, K., Alvarez-Martinez, O., Garza-Rodríguez, L., Martínez-Rodríguez, H., Bosques-Padilla, F., Ramos-Jiménez, J., Barrera-Saldaña, H., Rincón-Sánchez, A. R., and Rivas-Estilla, A. M. (2007) *J. Viral Hepat.* **14,** 608–617
9. Moradpour, D., Penin, F., and Rice, C. M. (2007) *Nat. Rev. Microbiol.* **5,** 453–463
10. Choi, J., Forman, H. J., Ou, J. H., Lai, M. M., Seronello, S., and Nandipati, A. (2006) *Free Radic. Biol. Med.* **41,** 1488–1498
11. Choi, J., Lee, K. J., Zheng, Y., Yamaga, A. K., Lai, M. M., and Ou, J. H. (2004) *Hepatology* **39,** 81–89
12. Huang, H., Chen, Y., and Ye, J. (2007) *Proc. Natl. Acad. Sci. U.S.A.* **104,** 18666–18670
13. Yano, M., Ikeda, M., Abe, K., Dansako, H., Ohkoshi, S., Aoyagi, Y., and Kato, N. (2007) *Antimicrob. Agents Chemother.* **51,** 2016–2027
14. Kuroki, M., Ariumi, Y., Ikeda, M., Dansako, H., Wakita, T., and Kato, N. (2009) *J. Virol.* **83,** 2338–2348
15. Kato, T., Date, T., Miyamoto, M., Sugiyama, M., Tanaka, Y., Orito, E., Ohno, T., Sugihara, K., Hasegawa, I., Fujiwara, K., Ito, K., Ozasa, A., Mizokami, M., and Wakita, T. (2005) *J. Clin. Microbiol.* **43,** 5679–5684
16. Wakita, T., Pietschmann, T., Kato, T., Date, T., Miyamoto, M., Zhao, Z., Murthy, K., Habermann, A., Kräusslich, H. G., Mizokami, M., Bartenschlager, R., and Liang, T. J. (2005) *Nat. Med.* **11,** 791–796
17. Blight, K. J., Kolykhalov, A. A., and Rice, C. M. (2000) *Science* **290,** 1972–1974
18. Blight, K. J., McKeating, J. A., and Rice, C. M. (2002) *J. Virol.* **76,** 13001–13014
19. Chang, T. K., Crespi, C. L., and Waxman, D. J. (1998) *Methods Mol. Biol.* **107,** 147–152
20. Eysseric, H., Gonthier, B., Soubeyran, A., Bessard, G., Saxod, R., and Barret, L. (1997) *Alcohol* **14,** 111–115
21. Shin, H. R. (2006) *Intervirology* **49,** 18–22
22. Marshall, D. J., Heisler, L. M., Lyamichev, V., Murvine, C., Olive, D. M., Ehrlich, G. D., Neri, B. P., and de Arruda, M. (1997) *J. Clin. Microbiol.* **35,** 3156–3162
23. Honda, M., Kaneko, S., Matsushita, E., Kobayashi, K., Abell, G. A., and Lemon, S. M. (2000) *Gastroenterology* **118,** 152–162
24. Cederbaum, A. I. (1991) *Alcohol Alcohol Suppl* **1,** 291–296
25. Adachi, J., Mizoi, Y., Fukunaga, T., Ogawa, Y., and Imamichi, H. (1989) *Alcohol Clin. Exp. Res.* **13,** 601–604
26. Clemens, D. L., Forman, A., Jerrells, T. R., Sorrell, M. F., and Tuma, D. J. (2002) *Hepatology* **35,** 1196–1204
27. Kalapos, M. P. (1999) *Med. Hypotheses* **53,** 236–242
28. Lieber, C. S. (2004) *Alcohol* **34,** 9–19
29. Ye, J. (2007) *PLoS Pathog* **3,** e108
30. Sagan, S. M., Rouleau, Y., Leggiadro, C., Supekova, L., Schultz, P. G., Su, A. I., and Pezacki, J. P. (2006) *Biochem. Cell Biol.* **84,** 67–79
31. Gretch, D., Corey, L., Wilson, J., dela Rosa, C., Willson, R., Carithers, R., Jr., Busch, M., Hart, J., Sayers, M., and Han, J. (1994) *J. Infect. Dis.* **169,** 1219–1225
32. Hosogaya, S., Ozaki, Y., Enomoto, N., and Akahane, Y. (2006) *Transl. Res.* **148,** 79–86
33. Plumlee, C. R., Lazaro, C. A., Fausto, N., and Polyak, S. J. (2005) *Virol. J.* **2,** 89
34. Gale, M., Jr., and Foy, E. M. (2005) *Nature* **436,** 939–945
35. Bader, T., Fazili, J., Madhoun, M., Aston, C., Hughes, D., Rizvi, S., Seres, K., and Hasan, M. (2008) *Am. J. Gastroenterol.* **103,** 1383–1389
36. Sheikh, M. Y., Choi, J., Qadri, I., Friedman, J. E., and Sanyal, A. J. (2008) *Hepatology* **47,** 2127–2133
37. Badawy, A. A. (1977) *Alcohol Alcohol* **12,** 120–136
38. Adiels, M., Boren, J., Caslake, M. J., Stewart, P., Soro, A., Westerbacka, J., Wennberg, B., Olofsson, S. O., Packard, C., and Taskinen, M. R. (2005) *Arterioscler. Thromb. Vasc. Biol.* **25,** 1697–1703
39. Towle, H. C. (1995) *J. Biol. Chem.* **270,** 23235–23238
40. Yano, M., Ikeda, M., Abe, K. I., Kawai, Y., Kuroki, M., Mori, K., Dansako, H., Ariumi, Y., Ohkoshi, S., Aoyagi, Y., and Kato, N. (2009) *Hepatology* **50,** 678–688

JOURNAL OF CLINICAL MICROBIOLOGY, Dec. 2009, p. 4141–4143 Vol. 47, No. 12
0095-1137/09/$12.00 doi:10.1128/JCM.01437-09

Evaluation of Hepatitis C Virus Core Antigen Assays in Detecting Recombinant Viral Antigens of Various Genotypes[▽]

Mohsan Saeed,[1,3] Ryosuke Suzuki,[1] Madoka Kondo,[1] Hideki Aizaki,[1] Takanobu Kato,[1] Toshiaki Mizuochi,[2] Takaji Wakita,[1] Haruo Watanabe,[1,3] and Tetsuro Suzuki[1]*

Department of Virology II[1] and Department of Safety Research on Blood and Biological Products,[2] National Institute of Infectious Diseases, Tokyo 162-8640, and Department of Infection and Pathology, Graduate School of Medicine, The University of Tokyo, Hongo, Bunkyo-ku, Tokyo 113-0033,[3] Japan

Received 24 July 2009/Returned for modification 3 September 2009/Accepted 19 September 2009

A single substitution within the hepatitis C virus core antigen sequence, A48T, which is observed in ~30% of individuals infected with genotype 2a virus, reduces the sensitivity of a commonly used chemiluminescence enzyme immunoassay. Quantitation of the antigen is improved by using a distinct anticore antibody with a different epitope.

Hepatitis C virus (HCV) is a major cause of chronic liver disease throughout the world. Accurate diagnosis of HCV infection is important due to the morbidity associated with the virus, and determining the level of viral replication is important in predicting and monitoring the effect of antiviral treatment. Although quantifying viral RNA represents the standard method for identifying active infection (5, 8, 13), several sensitive immunoassays that detect the viral core antigen (Ag) have now been developed as an alternative to HCV RNA testing (3, 4, 6, 9, 10, 12, 16). The amino acid sequence of the core Ag is largely conserved among different viral isolates (14); however, genetic variability of the virus constitutes one of the major challenges to using core Ag assays for diagnosis. In this study, we examined the effects of sequence heterogeneity on the sensitivity of diagnostic kits for detection of the core Ag by using recombinant Ag derived from each of the major HCV genotypes. Expression plasmids for epitope-tagged core Ag were generated by inserting cDNA for the full-length core region of genotype 1a (17; GenBank accession no. AF011751), 1b (1; D89815), 2a (7; AB047639), 2b (AB030907), or 3a virus, with a FLAG tag sequence attached at its 5′ end, into the EcoRI site of the pCAG mammalian expression vector (11). HEK293T cells transiently transfected with the expression plasmids were harvested 48 h after transfection using a passive lysis buffer (Promega, Madison, WI). Centrifugation was performed to remove the debris after ultrasonication. Total protein was quantified in aliquots of cell lysate by using the bicinchoninic acid method (Pierce, Rockford, IL) and then used for determining the concentrations of HCV core Ag.

Figure 1A shows comparable levels of core Ag in each sample of cell lysate, as determined by immunoblotting with anti-FLAG antibody (Ab). The ability of HCV core Ag assays to detect five different HCV genotypes were compared using a commercially available chemiluminescence enzyme immunoassay (CLEIA) (Lumipulse II HCV core assay [assay detection range, approximately 50 to 50,000 fmol/liter]; Fujirebio, Japan) (15) and enzyme-linked immunosorbent assay (ELISA) (Ortho HCV Ag ELISA test [assay detection range, approximately 44.4 to 3,600 fmol/liter]; Ortho-Clinical Diagnostics, Japan) (2) to detect HCV core Ag in cell lysate. As shown in Fig. 1B,

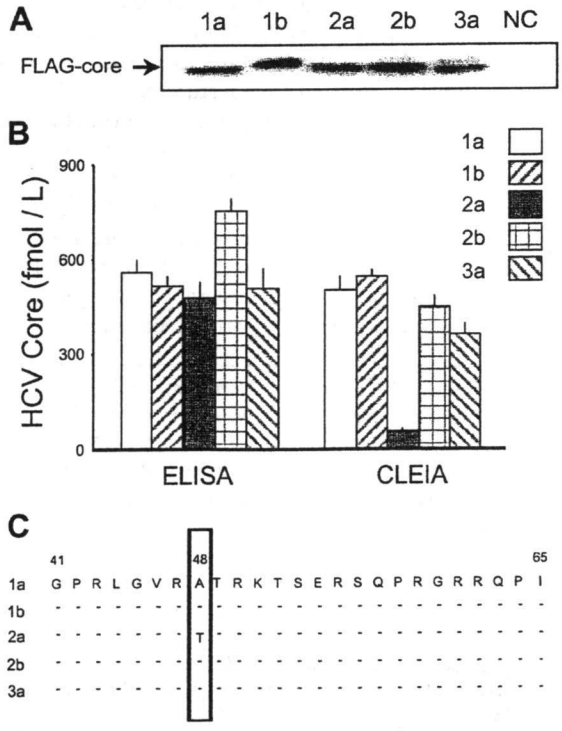

FIG. 1. Detection of recombinant HCV core Ag derived from genotype 1a, 1b, 2a, 2b, and 3a isolates by immunoblotting using an anti-FLAG Ab (A) as well as ELISA and CLEIA (B). The data shown in panel B represent the mean values and standard deviations ($n = 3$). NC, negative control. (C) The amino acid sequence from amino acids 41 to 65 of the core Ag used in this study. Key residues at the 48th position are boxed. Hyphens indicate conservation.

* Corresponding author. Mailing address: Department of Virology II, National Institute of Infectious Diseases, 1-23-1 Toyama, Shinjuku-ku, Tokyo 162-8640, Japan. Phone: 81-3-5285-1111. Fax: 81-3-5285-1161. E-mail: tesuzuki@nih.go.jp.

▽ Published ahead of print on 7 October 2009.

TABLE 1. Comparison of the 48th residues of HCV core Ags of genotypes 1a, 1b, 2a, 2b, and 3a

Genotype	No. of isolates	No. (%) of isolates with residue at 48th position		
		T	A	Other
1a	263	9 (3.5)	254 (96.5)	0 (0)
1b	298	2 (0.7)	294 (98.6)	2 (0.7)
2a	17	5 (29.5)	12 (70.5)	0 (0)
2b	17	0 (0)	17 (100)	0 (0)
3a	23	0 (0)	23 (100)	0 (0)
Total	618	16 (2.6)	600 (97.1)	2 (0.3)

although the ELISA measured similar concentrations of core Ag in all samples, apparent low levels of the genotype 2a core Ag, originally from an isolate known as the JFH-1 isolate (7), were detected using the CLEIA method, suggesting that some differences in the amino acid sequences corresponding to particular HCV genotypes or isolates may influence the sensitivity of core Ag detection. A comparison of the core Ag sequences, including the monoclonal Ab epitopes used in the development of CLEIA, revealed conservation of alanine at the 48th position in four clones, of genotypes 1a, 1b, 2b, and 3a, but not genotype 2a, for which there is a threonine at this position (Fig. 1C). Based on our analysis of sequences available from the HCV database (http://hcv.lanl.gov/content/sequence/NEWALIGN/align.html), alanine is highly conserved at the 48th residue of the core Ag for HCV isolates of genotypes 1a, 1b, 2b, and 3a (Table 1). In contrast, alanine and threonine occur in this position in 70.5% and 29.5%, respectively, of genotype 2a isolates. To examine whether the low sensitivity of the CLEIA method might be due to this particular amino acid change, we next replaced threonine with alanine at the 48th position of the JFH-1 core Ag (for

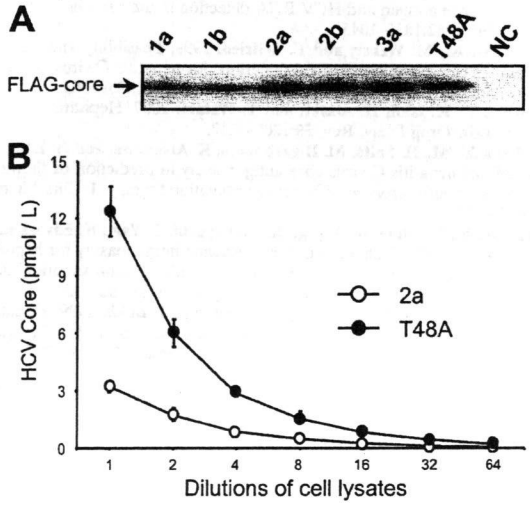

FIG. 2. Effect of T48A substitution in the core Ag of the JFH-1 isolate with regard to sensitivity of the CLEIA method. Samples of wild-type or mutated core Ag cell lysate were analyzed by immunoblotting (A) and CLEIA (B). The data shown in panel B represent the mean values and standard deviations (n = 3). NC, negative control.

TABLE 2. Comparison of the modified CLEIA with the original version for detection of the core Ags of genotypes 1a, 1b, 2a, 2b, and 3a[a]

Genotype	CLEIA	HCV core antigen concn (fmol/liter) in serially diluted cell lysates at indicated fold dilution							
		1	2	4	8	16	32	64	128
1a	Original	11,147	5,527	2,611	1,484	691	403	195	101
	Modified	10,511	5,700	2,676	1,420	716	444	200	111
1b	Original	11,612	5,618	3,081	1,551	779	409	223	113
	Modified	11,192	6,028	2,824	1,522	804	431	197	101
2a	Original	3,216	1,710	844	480	232	104	48	36
	Modified	12,101	6,255	3,153	1,676	805	422	212	106
2b	Original	10,559	5,635	2,811	1,286	762	387	194	94
	Modified	10,977	6,179	3,381	1,624	842	437	219	129
3a	Original	11,478	5,891	2,922	1,414	756	422	212	112
	Modified	11,208	6,225	3,126	1,555	791	445	215	100

[a] Data represent the mean values in triplicate measurements.

the mutant JFH-1coreT48A) and measured the HCV core Ag concentration in cells expressing both mutated and wild-type JFH-1 core Ag. After confirming comparable levels of FLAG-tagged core Ag in the cell lysate samples by immunoblotting (Fig. 2A), HCV core Ag was quantified in the samples by serial dilution via the CLEIA method. As shown in Fig. 2B, the core Ag concentrations of JFH-1coreT48A were assessed to be 3.2- to 3.8-fold higher than those of the wild-type core Ag, suggesting that the sensitivity of HCV core Ag detection may have been affected by the 48th residue in the core Ag. Data for samples derived from genotypes 1a, 1b, 2b, and 3a were analogous to data for JFH-1coreT48A (data not shown). Although HCV isolates with threonine at the 48th position of the core Ag sequence comprise a relatively small proportion of the major genotype population, only 2.6% of the genotype 1a, 1b, 2a, 2b, and 3a isolates here (16 of 618 isolates; Table 1), attempts to overcome this problem would improve the overall sensitivity and usefulness of the assay. To achieve this aim, another monoclonal anticore Ab, whose epitope is comprised of amino acids 50 to 65, which are completely conserved among all the genotypes examined (Fig. 1C), was therefore used as a second Ab in a modified version of the CLEIA. We compared this modified assay with the original version by measurement of core Ag concentrations of the various genotypes (Fig. 2A) as illustrated in Table 2. The modified assay was able to quantify core Ag from genotypes 1a, 1b, 2a, 2b, and 3a with no significant differences observed between Ag levels in samples from different genotypes at each dilution.

It has been demonstrated that the HCV core Ag assay is a useful alternative to HCV RNA quantification for the diagnosis of hepatitis C and for monitoring the antiviral effects of treatment. Compared to various reverse transcription-PCR methods, HCV core assays are less expensive and easier to perform, without the requirement of sophisticated laboratory equipment and specially trained laboratory personnel. In addition, the core Ag assay can be used to measure a more diverse set of blood samples, such as sera stored for a long period of time, because the viral Ag is generally more stable than the RNA in sera or plasma. Despite the adequate performance of core Ag assays, we have shown that a single amino acid substitution at the 48th position of the core Ag changes the detection sensitivity. It is also noted that, although the original CLEIA should be improved, the ELISA used in this study may be substituted for it.

In conclusion, we have identified a distinct anticore Ab with a different epitope that might enable improved detection across all of the major HCV isolates. The findings of this study would provide useful information for the development of an improved assay with greater accuracy.

We thank Ortho-Clinical Diagnostics K.K. and Fujirebio Inc. for providing the diagnostic kits and for helping us in performing the assays.

This work was supported by a grant-in-aid for scientific research from the Ministry of Health, Labor and Welfare of Japan.

REFERENCES

1. **Aizaki, H., Y. Aoki, T. Harada, K. Ishii, T. Suzuki, S. Nagamori, G. Toda, Y. Matsuura, and T. Miyamura.** 1998. Full-length complementary DNA of hepatitis C virus genome from an infectious blood sample. Hepatology **27:** 621–627.
2. **Aoyagi, K., C. Ohue, K. Iida, T. Kimura, E. Tanaka, K. Kiyosawa, and S. Yagi.** 1999. Development of a simple and highly sensitive enzyme immunoassay for hepatitis C virus core antigen. J. Clin. Microbiol. **37:**1802–1808.
3. **Bouvier-Alias, M., K. Patel, H. Dahari, S. Beaucourt, P. Larderie, L. Blatt, C. Hezode, G. Picchio, D. Dhumeaux, A. U. Neumann, J. G. McHutchison, and J. M. Pawlotsky.** 2002. Clinical utility of total HCV core antigen quantification: a new indirect marker of HCV replication. Hepatology **36:**211–218.
4. **Buti, M., C. Mendez, M. Schaper, S. Sauleda, A. Valdes, F. Rodriguez-Frias, R. Jardi, and R. Esteban.** 2004. Hepatitis C virus core antigen as a predictor of non-response in genotype 1 chronic hepatitis C patients treated with peginterferon alpha-2b plus ribavirin. J. Hepatol. **40:**527–532.
5. **Chevaliez, S., and J. M. Pawlotsky.** 2007. Practical use of hepatitis C virus kinetics monitoring in the treatment of chronic hepatitis C. J. Viral Hepat. **14** (Suppl. 1):77–81.
6. **González, V., E. Padilla, M. Diago, M. D. Gimenez, R. Sola, L. Matas, S. Montoliu, R. M. Morillas, C. Perez, and R. Planas.** 2005. Clinical usefulness of total hepatitis C virus core antigen quantification to monitor the response to treatment with peginterferon alpha-2a plus ribavirin. J. Viral Hepat. **12:**481–487.
7. **Kato, T., A. Furusaka, M. Miyamoto, T. Date, K. Yasui, J. Hiramoto, K. Nagayama, T. Tanaka, and T. Wakita.** 2001. Sequence analysis of hepatitis C virus isolated from a fulminant hepatitis patient. J. Med. Virol. **64:**334–339.
8. **Laperche, S.** 2005. Blood safety and nucleic acid testing in Europe. Euro Surveill. **10:**3–4.
9. **Maynard, M., P. Pradat, P. Berthillon, G. Picchio, N. Voirin, M. Martinot, P. Marcellin, and C. Trepo.** 2003. Clinical relevance of total HCV core antigen testing for hepatitis C monitoring and for predicting patients' response to therapy. J. Viral Hepat. **10:**318–323.
10. **Netski, D. M., X. H. Wang, S. H. Mehta, K. Nelson, D. Celentano, S. Thongsawat, N. Maneekarn, V. Suriyanon, J. Jittiwutikorn, D. L. Thomas, and J. R. Ticehurst.** 2004. Hepatitis C virus (HCV) core antigen assay to detect ongoing HCV infection in Thai injection drug users. J. Clin. Microbiol. **42:**1631–1636.
11. **Niwa, H., K. Yamamura, and J. Miyazaki.** 1991. Efficient selection for high-expression transfectants with a novel eukaryotic vector. Gene **108:**193–199.
12. **Nübling, C. M., G. Unger, M. Chudy, S. Raia, and J. Lower.** 2002. Sensitivity of HCV core antigen and HCV RNA detection in the early infection phase. Transfusion **42:**1037–1045.
13. **Roth, W. K., M. Weber, and E. Seifried.** 1999. Feasibility and efficacy of routine PCR screening of blood donations for hepatitis C virus, hepatitis B virus, and HIV-1 in a blood-bank setting. Lancet **353:**359–363.
14. **Suzuki, T., K. Ishii, H. Aizaki, and T. Wakita.** 2007. Hepatitis C viral life cycle. Adv. Drug Deliv. Rev. **59:**1200–1212.
15. **Takahashi, M., H. Saito, M. Higashimoto, K. Atsukawa, and H. Ishii.** 2005. Benefit of hepatitis C virus core antigen assay in prediction of therapeutic response to interferon and ribavirin combination therapy. J. Clin. Microbiol. **43:**186–191.
16. **Tanaka, E., C. Ohue, K. Aoyagi, K. Yamaguchi, S. Yagi, K. Kiyosawa, and H. J. Alter.** 2000. Evaluation of a new enzyme immunoassay for hepatitis C virus (HCV) core antigen with clinical sensitivity approximating that of genomic amplification of HCV RNA. Hepatology **32:**388–393.
17. **Yanagi, M., R. H. Purcell, S. U. Emerson, and J. Bukh.** 1999. Hepatitis C virus: an infectious molecular clone of a second major genotype (2a) and lack of viability of intertypic 1a and 2a chimeras. Virology **262:**250–263.

Journal of General Virology (2010), 91, 122–132 DOI 10.1099/vir.0.015909-0

Requirement of cellular DDX3 for hepatitis C virus replication is unrelated to its interaction with the viral core protein

Allan G. N. Angus,[1] David Dalrymple,[1] Steeve Boulant,[1] David R. McGivern,[2] Reginald F. Clayton,[1] Martin J. Scott,[1] Richard Adair,[1] Susan Graham,[1] Ania M. Owsianka,[1] Paul Targett-Adams,[1] Kui Li,[3] Takaji Wakita,[4] John McLauchlan,[1] Stanley M. Lemon[2] and Arvind H. Patel[1]

Correspondence
Arvind H. Patel
a.patel@mrcvu.gla.ac.uk

[1]MRC Virology Unit, Institute of Virology, University of Glasgow, Church Street, Glasgow G11 5JR, UK

[2]Center for Hepatitis Research, Institute for Human Infections & Immunity, and the Department of Microbiology and Immunology, University of Texas Medical Branch, Galveston, TX 77555-0610, USA

[3]Department of Molecular Sciences, University of Tennessee Health Science Center, Memphis, TN 38163, USA

[4]Department of Virology II, National Institute of Infectious Diseases, Tokyo, Japan

The cellular DEAD-box protein DDX3 was recently shown to be essential for hepatitis C virus (HCV) replication. Prior to that, we had reported that HCV core binds to DDX3 in yeast-two hybrid and transient transfection assays. Here, we confirm by co-immunoprecipitation that this interaction occurs in cells replicating the JFH1 virus. Consistent with this result, immunofluorescence staining of infected cells revealed a dramatic redistribution of cytoplasmic DDX3 by core protein to the virus assembly sites around lipid droplets. Given this close association of DDX3 with core and lipid droplets, and its involvement in virus replication, we investigated the importance of this host factor in the virus life cycle. Mutagenesis studies located a single amino acid in the N-terminal domain of JFH1 core that when changed to alanine significantly abrogated this interaction. Surprisingly, this mutation did not alter infectious virus production and RNA replication, indicating that the core–DDX3 interaction is dispensable in the HCV life cycle. Consistent with previous studies, siRNA-led knockdown of DDX3 lowered virus production and RNA replication levels of both WT JFH1 and the mutant virus unable to bind DDX3. Thus, our study shows for the first time that the requirement of DDX3 for HCV replication is unrelated to its interaction with the viral core protein.

Received 17 August 2009
Accepted 25 September 2009

INTRODUCTION

Persistent hepatitis C virus (HCV) infection is a major cause of chronic hepatitis, cirrhosis and hepatocellular carcinoma (HCC). Current treatments for chronic infection are ineffective in approximately 50% of patients (Chen & Morgan, 2006). The virus, which belongs to the family *Flaviviridae*, has a positive-sense RNA genome encoding a polyprotein that is cleaved by cellular and viral proteases to yield mature structural and non-structural proteins. The structural proteins are core and the envelope glycoproteins E1 and E2, while the non-structural proteins are p7, NS2, NS3, NS4A, NS4B, NS5A and NS5B (reviewed by Moradpour *et al.*, 2007). HCV exhibits a high degree of genetic variability with six distinct viral genotypes, each further divided into subtypes, and within a single individual the virus exists as a constantly evolving quasispecies (Bukh *et al.*, 1995; Pawlotsky, 2003; Simmonds, 1995).

HCV core is a highly conserved basic, RNA-binding protein that forms the viral nucleocapsid (McLauchlan, 2000). Mature core is a dimeric, alpha-helical protein that can be separated into two domains (D1 and D2) based on its hydropathic profile (Boulant *et al.*, 2005; McLauchlan, 2000). The N-terminal hydrophilic D1 domain consists of the first 117 aa and is mainly involved in RNA binding and oligomerization of the core protein (Boulant *et al.*, 2005).

Supplementary figures are available with the online version of this paper.

In addition, D1 also interacts with several cellular factors (McLauchlan, 2000). The hydrophobic D2 domain, which spans amino acid residues 118 to approximately 169, is required for correct folding of D1. D2 consists of two amphipathic α-helices connected by a hydrophobic loop and mediates core association with lipid droplets (LDs) and endoplasmic reticulum membranes (Barba *et al.*, 1997; Boulant *et al.*, 2006; Hope & McLauchlan, 2000). Recent evidence strongly suggests that the HCV core–LD association is important for the production of infectious virus particles (Boulant *et al.*, 2007; Miyanari *et al.*, 2007; Shavinskaya *et al.*, 2007).

We and others previously showed that the core domain D1 interacts with the cellular DEAD-box RNA helicase DDX3 (Mamiya & Worman, 1999; Owsianka & Patel, 1999; You *et al.*, 1999). In mammalian cells, DDX3 is present throughout the cytoplasm and can also be found in the nucleus. Ectopic expression of HCV core in these cells results in the redistribution of a proportion of DDX3 to distinct cytoplasmic sites, where it co-localizes with core. Indeed, DDX3 was recently shown to be present on LDs in core-expressing Hep39 cells (Sato *et al.*, 2006).

Cellular RNA helicases of the DEAD-box family participate in all biological processes involving RNA. They possess nine conserved motifs (see Fig. 1), including motif II (Asp–Glu–Ala–Asp or DEAD) after which the protein family is named (reviewed by Cordin *et al.*, 2006; Rocak & Linder, 2004). DDX3 is a ubiquitous cellular protein, possessing ATPase and helicase activities (Franca *et al.*, 2007; Yedavalli *et al.*, 2004). Known homologues include murine PL10 (Leroy *et al.*, 1989), *Xenopus laevis* An3 (Gururajan *et al.*, 1991) and yeast Ded1 (Jamieson & Beggs, 1991). The exact cellular function of DDX3 has yet to be defined, but there is evidence for its involvement in splicing (Deckert *et al.*, 2006; Zhou *et al.*, 2002), translation initiation and repression (Beckham *et al.*, 2008; Shih *et al.*, 2008), cell cycle regulation (Chang *et al.*, 2006; Chao *et al.*, 2006; Huang *et al.*, 2004; Sekiguchi *et al.*, 2007), nucleocytoplasmic RNA shuttling (Yedavalli *et al.*, 2004), RNA transport (Kanai *et al.*, 2004), interferon induction (Schroder *et al.*, 2008; Soulat *et al.*, 2008) and apoptosis (Sun *et al.*, 2008). Both upregulation and downregulation of DDX3 have been reported in various tumour tissues, suggesting divergent roles of DDX3 in cancer-related pathogenesis (Botlagunta *et al.*, 2008; Chang *et al.*, 2006; Chao *et al.*, 2006; Huang *et al.*, 2004).

Previously, we proposed that the HCV core–DDX3 interaction might function in virus replication and/or pathogenesis (Owsianka & Patel, 1999). Two separate studies recently provided evidence for the involvement of DDX3 in HCV replication (Ariumi *et al.*, 2007; Randall *et al.*, 2007). The importance of DDX3 in the life cycle of other viruses has also become apparent, including its requirement for human immunodeficiency virus-1 (HIV-1) replication (Yedavalli *et al.*, 2004). Furthermore, the DDX3 homologue Ded1 is required for brome mosaic virus replication (Noueiry *et al.*, 2000). In contrast, DDX3 inhibits hepatitis B virus transcription by its incorporation into nucleocapsids (Wang *et al.*, 2009). Thus, there is increasing evidence that DDX3 is important in the life cycle of several diverse viruses.

The direct relevance of the core–DDX3 interaction for the HCV life cycle has not yet been elucidated. In this study, we show that this interaction does occur in cultured cells infected with HCV strain JFH1 (Wakita *et al.*, 2005), and that DDX3 co-localizes directly with core on LDs. Using alanine substitution mutagenesis, we identified a key amino acid residue within the D1 domain of core that is

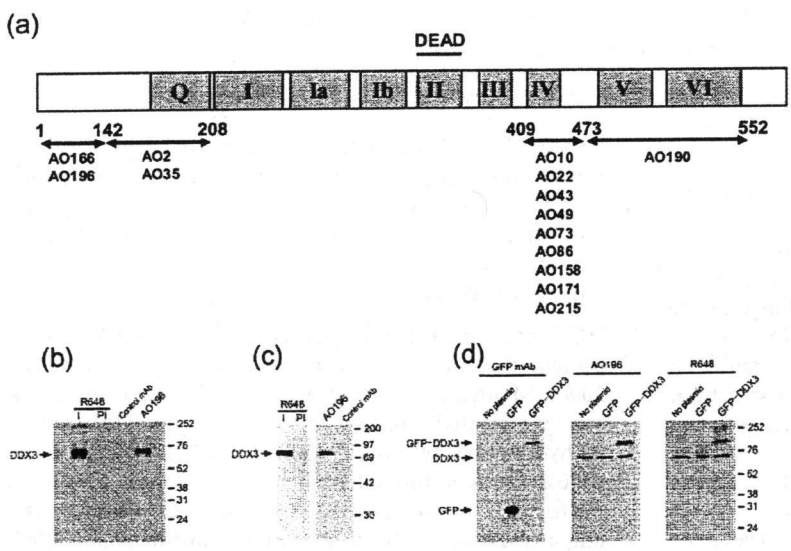

Fig. 1. Generation of anti-DDX3 antibodies. (a) Schematic representation of DDX3 protein structure showing the nine conserved motifs, including motif II (or the DEAD motif). The arrows mark the epitopes recognized by the mouse mAbs. (b) Characterization of anti-DDX3 antibodies. HuH-7 cell lysates were immunoprecipitated with the immune (I) and pre-immune (PI) antiserum R648, or mAb AO196 or an isotype control mAb. The immune complexes were analysed by Western blotting using biotinylated R648. Positions of molecular mass markers are shown (in kDa). (c) Western blotting of HuH-7 cell lysates with R648-I, -PI, mAb AO196 and isotype control mAb. (d) Western blotting of lysates of HEK cells transfected with a plasmid expressing EGFP alone or an EGFP–DDX3 fusion protein using anti-GFP mAb, AO196 and R648.

critical for this interaction. Furthermore, we examine the impact of abrogation of the core–DDX3 interaction on virus RNA replication and infectious progeny yields in cultured cells.

RESULTS

Generation of DDX3 antibodies

We previously showed that DDX3 co-localizes with HCV genotype 1a core in cytoplasmic punctate spots (Owsianka & Patel, 1999). To better understand the nature of this interaction, we generated several mouse mAbs (prefixed with 'AO', see Fig. 1a) and two rabbit polyclonal antisera (R647 and R648) to human DDX3. Both rabbit antisera and the majority of mAbs were found to interact with DDX3 by ELISA, Western blotting and immunoprecipitation assays (data not shown). The epitopes of mAbs reactive to DDX3 in Western blots were broadly mapped using truncated forms of DDX3 expressed in bacteria as GST-fusion proteins. Most of the mAbs recognized aa 409–473, a region located between motifs III and V of DDX3, whereas mAb AO190 recognized motifs V and VI. mAbs AO166 and AO196 bound to the N-terminal region, whereas mAbs AO2 and AO35 recognized the region downstream preceding the ATPase domain of DDX3 (Fig. 1a).

The specificities of antibodies AO196 and R648 for DDX3 in immunoprecipitation and Western blot assays are shown in Fig. 1(b, c, d). The polyclonal serum R648 (but not the pre-immune control serum) specifically immunoprecipitated DDX3 from a cytoplasmic extract of HuH-7 cells, as did mAb AO196 (Fig. 1b). R648 and AO196 also recognized DDX3 in cytoplasmic extracts of HuH-7 cells by Western blotting (Fig. 1c). The specificity of these antibodies was further demonstrated by their recognition of both endogenous DDX3 and an enhanced green fluorescent protein (EGFP)–DDX3 fusion protein expressed in HEK cells (Fig. 1d). mAb AO196 and R648 recognized only the cytoplasmic form of DDX3 by immunofluorescence (Fig. 2a and data not shown), even though they were able to detect DDX3 in the nuclear extracts of cells in both immunoprecipitation and Western blotting assays (data not shown). In contrast, another mAb

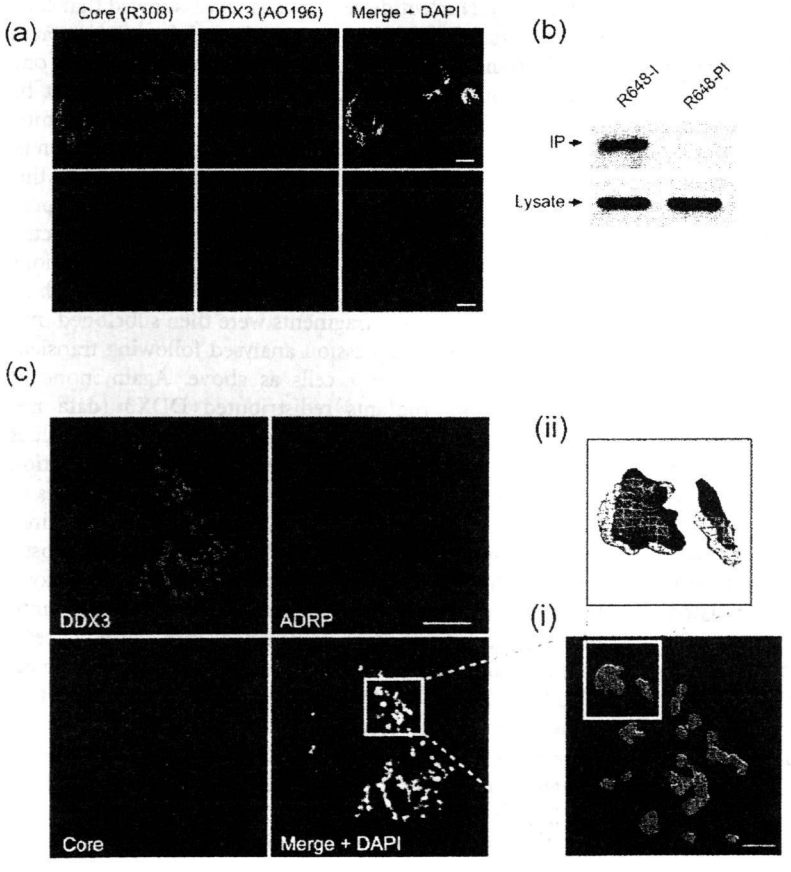

Fig. 2. Sequestration of DDX3 by HCV core. (a) DDX3 co-localizes with core in JFH1-infected cells. HuH-7 cells were either mock-infected (lower panel) or infected with JFH1 (top panel). At 3 days post-infection, cells were fixed and probed with HCV core and DDX3 using antibodies R308 and A0196, respectively. Cell nuclei were detected by counterstaining with DAPI. (b) Co-immunoprecipitation of core by anti-DDX3 antiserum. HuH-7 cells electroporated with viral RNA were lysed at 72 h post-incubation, and the lysate immunoprecipitated with anti-DDX3 R648 immune (I) or pre-immune (PI) serum. The resulting precipitates were examined by immunoblotting using anti-core mAb c7-50 (top panel). One twentieth of the cell lysate used in the co-immunoprecipitation assay was immunoblotted for core with mAb c7-50 as the input control (bottom panel). (c) Localization of DDX3 and core on LDs. HuH-7 cells electroporated with the $JFH1_{WT}$ RNA were fixed at 72 h post-transfection and probed using antibodies to core (R308), DDX3 (AO196) and ADRP. Z-stack analysis of all three proteins was performed by recording a series of approximately 20 images. 3D reconstructions of the boxed areas are shown (i) and a selected area is shown in greater detail (ii) where DDX3 is depicted as a wire frame to reveal the core–ADRP association. Bars, 10 μm for confocal images and 2 μm for 3D image.

designated AO322 recognized both the cytoplasmic and the nuclear form of DDX3 by immunofluoresence (Supplementary Fig. S1a).

HCV core interacts with cellular DDX3 in cells replicating WT JFH1

The core–DDX3 interaction was previously demonstrated in cells ectopically expressing HCV genotype 1a core, and in the absence of virus RNA replication and productive infection (Owsianka & Patel, 1999). To test whether DDX3 interacts with JFH1 core, HuH-7 cells transfected with virus RNA were first analysed by indirect immunofluorescence. DDX3 was found to be sequestered by core in JFH1-replicating cells as detected using mAbs AO196 and AO322 [Fig. 2a and Supplementary Fig. S1a (available in JGV Online), respectively]. It should be noted that the core-bound DDX3 emitted a stronger fluorescent signal compared with free DDX3 occupying the cell cytoplasm. Thus, adjustment of the core-bound DDX3 signal to prevent overexposure resulted in the apparent loss of free DDX3 from the image. A representative image of core and DDX3 in virus-infected and surrounding non-infected cells taken at two different intensities is shown in Supplementary Fig. S1(b) (available in JGV Online). The anti-DDX3 antiserum R648 specifically co-immunoprecipitated core from JFH1-replicating cells, further confirming a direct interaction between these two proteins (Fig. 2b).

We also found that DDX3 co-localized with core protein in the NNeo/C-5B(+) cell line harbouring an autonomously replicating genome-length genotype 1b RNA (Ikeda *et al.*, 2002), and HuH-7 cells infected with the intergenotypic 1a/2a chimeric virus [H-NS2/NS3 J(YH/QL)] (Yi *et al.*, 2007) (Supplementary Fig. S1c, d, available in JGV Online). Thus, the recruitment of DDX3 by core is in good agreement with our previous results (Owsianka & Patel, 1999), and is not limited to one virus genotype.

DDX3 interacts with HCV core on LDs

The association of HCV core with LDs is essential for infectious virus production (Boulant *et al.*, 2007; Miyanari *et al.*, 2007; Shavinskaya *et al.*, 2007). We sought to gain further insight into the core–DDX3 complex in the context of the JFH1 system by analysing the intracellular distribution of core and DDX3. HuH-7 cells electroporated with JFH1 RNA were analysed by indirect immunofluorescence for HCV core, DDX3 and adipocyte differentiation-related protein (ADRP), a protein abundant on the surface of LDs (Fujimoto *et al.*, 2004). As shown in Fig. 2(c) left, core associated with ADRP and the localization of DDX3 was precisely coincident with both proteins, indicating its redistribution to LDs. To examine the subcellular position of DDX3 and core in relation to ADRP in greater detail, a series of Z-stacks was obtained and used after blind deconvolution to create a three-dimensional model of LDs coated by core, ADRP and DDX3. As reported before (Boulant *et al.*, 2007), core fully coated LDs. We found that DDX3 by virtue of its interaction with core was also fully associated with LDs [Fig. 2c (i) and (ii)].

Identification of core residues required for DDX3 interaction

We previously reported that aa 1–59 of core protein are involved in its interaction with DDX3 (Owsianka & Patel, 1999). To identify critical residues within this region, a library of core 1–59 mutants containing single or multiple amino acid substitutions was generated by error-prone PCR (EP-PCR). The mutated sequences were fused in-frame with GFP and expressed in bacteria. The mutant fusion proteins were screened by incubation with GST–DDX3 fusion protein immobilized in ELISA wells, and the bound mutants detected using a rabbit polyclonal anti-GFP antiserum. Of 130 clones screened, only nine were found to be defective in binding to GST–DDX3 (data not shown). In order to confirm these results, all nine mutants were individually subcloned into a sequence encoding the HCV genotype 1a strain H77c core, E1 and E2 (pCE1E2) in a mammalian expression vector pcDNA3.1/Zeo+ (Invitrogen), and their expression was analysed by indirect immunofluorescence. The results were in accordance with the data from the initial ELISA screen in that all nine mutated core proteins failed to redistribute DDX3 (data not shown). Nucleotide sequence analysis showed that each of the mutants carried between one and four amino acid substitutions (Fig. 3). Of interest, mutant 90 had only one substitution (I30N), indicating that this residue must be required for the interaction of core with DDX3. All nine mutant proteins had at least one amino acid substitution in the region spanning residues 24–36, indicating that this region may harbour residues that are critical for the core–DDX3 interaction. To test this hypothesis, site-directed mutagenesis was carried out to revert any mutations outside of this 13 aa region back to the WT residue. These new mutant core 1–59 fragments were then subcloned into pCE1E2, and their expression analysed following transient transfection into HuH-7 cells as above. Again, none of these new core mutants redistributed DDX3 (data not shown), indicating that the 13 aa region between residues 24 and 36 of core is indeed involved in the interaction between core and DDX3. To determine which residues in this 13 aa region were essential, we carried out alanine-scanning mutagenesis across aa 24–36, individually substituting each residue in this region with alanine. As before, these alanine mutant sequences were subcloned into pCE1E2 and transiently transfected into HuH-7 cells. Immunofluorescence analysis revealed seven mutants (P25A, G26A, G28A, Q29A, V31A, G32A and L36A) that showed distinct co-localization between core and DDX3 (similar to that seen with WT HCV core), whilst the other mutants (F24A, G27A, I30A, G33A, V34A and Y35A) displayed no interaction with DDX3 at all (Supplementary Fig. S2, available in JGV Online). Thus, these results

	1 10 20 30 40 50 59
Core	MSTNPKPQPK TKRNTNRRPE DVKFPGGGQI VGGVYLLPRR GPRLGVRTTR KTSERSQPR
Mutant 25	--------K- ---------- ---------- ---G------ ---------- ------R--
Mutant 36	---------- ---------- ---------- ---D-----W ---------- -S-------
Mutant 90	---------- ---------- ---------N ---------- ---------- ---------
Mutant 99	---------- ---------- -D-------- ---D------ ---------- ---------
Mutant 110	---------- ---------- ---------N ---------- --S------- ---------
Mutant 111	-----E---- ---------- ---------- ----N----- ---------- ---------
Mutant 115	---------D -E-------- ---S------ ---------- ---------- ---------
Mutant 125	---------- -----I---- --------R- ----N----- ---------- ------R--
Mutant 126	-------H-- ---------- -----D---N -----W---- ---------- ---------

Fig. 3. Identification of core residues critical for its interaction with DDX3. Amino acid substitutions in residues 1–59 of core in nine mutants unable to interact with DDX3. Residues in the region 24–36 (shaded box) were targeted for alanine-scanning mutagenesis, which identified residues at positions 24, 27, 30, 33, 34 and 35 (underlined in the sequence at the top) that were critical for DDX3 interaction.

indicate that core residues F24, G27, I30, G33, V34 and Y35 are critical for its interaction with DDX3.

Disrupting the core–DDX3 interaction

Sequence comparison of core protein from strains H77c (genotype 1a) and JFH1 (genotype 2a) revealed 96.6% identity within the first 59 residues of core, with the key residues (F24, G27, I30, G33, V34 and Y35) for interaction with DDX3 being fully conserved (data not shown). Thus, recombinant JFH1 genomes each containing one of the six mutations were constructed. All mutants were replication competent as seen by the expression of NS5A protein at 3 days post-transfection (Fig. 4). The viral core protein in these cells was detected using two different anti-core antibodies, which bound to the mutant proteins with varying affinity. mAb c7-50 bound minimally or not at all to I30A and G33A mutants, but had increased affinity for the V34A protein. The anti-core rabbit serum R308 on the other hand recognized all core forms equally except for G33A (Fig. 4). Notably, all six core mutations are located within the epitope (aa 21–40) recognized by c7-50 (Moradpour *et al.*, 1996), which may account for the altered affinity of this mAb to some mutants. The antiserum R308 was raised against a peptide corresponding to core aa 5–25 (Hope & McLauchlan, 2000). Therefore, the smaller quantities of G33A core detected using R308 suggest either this mutation lowers the stability of the protein or simply reduces the binding efficiency of the antibody. Importantly, there was no detectable change in DDX3 protein levels in any of the transfected cell cultures tested (Fig. 4).

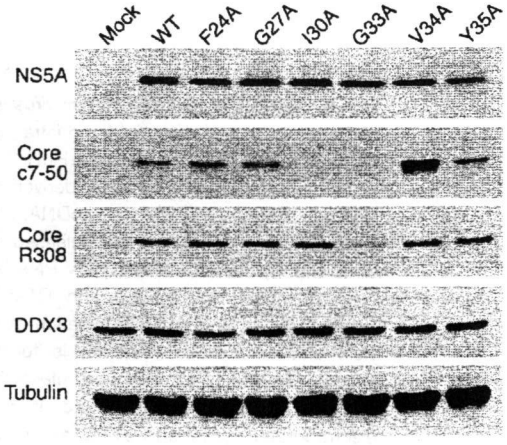

Fig. 4. Analysis of JFH1 core mutant viruses. HuH-7 cells electroporated with viral RNAs as shown were subjected to Western immunoblotting at 72 h post-incubation using anti-NS5a mAb 9E10, anti-core antibodies mAb c7-50 or R308, anti-DDX3 mAb AO196 and an anti-tubulin antibody.

We next tested by co-immunoprecipitation if these mutations had effectively disrupted the core–DDX3 interaction in virus-replicating cells. We excluded mutants I30A, G33A and V34A from this assay due to their altered affinity to mAb c7-50 (Fig. 4), which is the antibody we found to be most compatible in our co-immunoprecipitation assay. As shown in Fig. 5, the F24A and G27A core mutants were co-immunoprecipitated by the anti-DDX3 antiserum R648 in much lower amounts than the WT protein. However, the Y35A core was not co-immunoprecipated at all, indicating that its interaction with DDX3 was abrogated. Consistent with these findings, no co-localization of core and DDX3 was seen in cells replicating $JFH1_{Y35A}$ by immunofluoresence analysis (Fig. 5b). Importantly, this mutant core remained associated with LDs, which is not surprising since motifs responsible for targeting core to LDs are located in the D2 domain (Hope & McLauchlan, 2000).

HCV replication in the absence of the core–DDX3 interaction

To determine the importance of this interaction in the virus life cycle, we examined the phenotype of $JFH1_{Y35A}$.

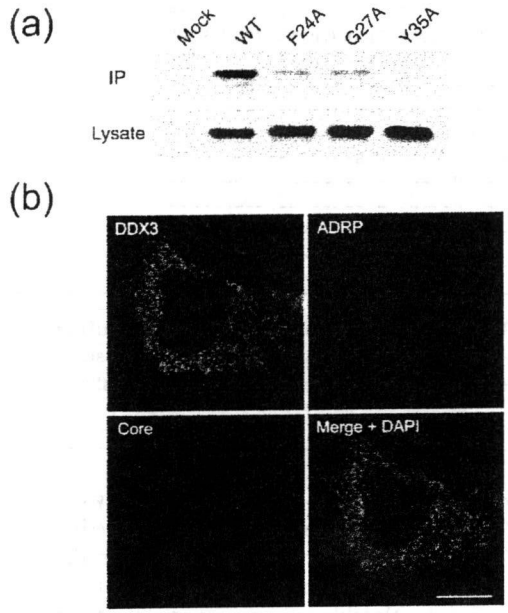

Fig. 5. Analysis of the interaction of DDX3 with core mutants. (a) HuH-7 cells were electroporated with different viral RNAs and HCV core co-immunoprecipitated at 72 h post-incubation using the anti-DDX3 serum R648 as described in the legend to Fig. 2b. (b) HuH-7 cells electroporated with $JFH1_{Y35A}$ were fixed at 72 h post-incubation and analysed by confocal microscopy for the intracellular distribution of core, DDX3 and ADRP using appropriate antibodies. Bar, 10 μm.

HuH-7 cells were electroporated with $JFH1_{WT}$, $JFH1_{Y35A}$ or the replication-deficient $JFH1_{GND}$ RNAs and incubated for various time points before determining the progeny virus yields released into the medium and intracellular viral RNA levels. As shown in Fig. 6(a), the number of infectious particles released by $JFH1_{Y35A}$-replicating cells was lower in comparison with $JFH1_{WT}$-transfected cells at 24 and 48 h post-transfection, although parity was achieved at 72 h. The intracellular RNA replication levels of $JFH1_{Y35A}$ were similar to $JFH1_{WT}$ throughout the time-course (Fig. 6b). As expected, no virus release or intracellular viral RNA replication was detected in cells harbouring $JFH1_{GND}$ RNA (Fig. 6a, b). We next examined the infectivity and replication of the core mutant virus released from electroporated cells. To do this, we infected naïve cells at an equal m.o.i. and quantified the released infectious virus progeny and the intracellular viral RNA at various times post-infection. As shown in Fig. 6(c, d), respectively, both the virus yields and RNA replication levels of $JFH1_{Y35A}$ were very similar to $JFH1_{WT}$. We found no direct reversion or second-site mutation in $JFH1_{Y35A}$ core sequence. Thus, our data indicate that the core–DDX3 interaction does not play a role in HCV morphogenesis.

Replication of HCV following siRNA-mediated knockdown of DDX3

Recent reports have shown that siRNA-mediated knockdown of DDX3 reduces $JFH1_{WT}$ replication in infected cells (Ariumi *et al.*, 2007; Randall *et al.*, 2007). To assess the influence of DDX3 abundance on virus infection in the absence of the core–DDX3 interaction, we measured the replication of $JFH1_{WT}$ and $JFH1_{Y35A}$ following infection of

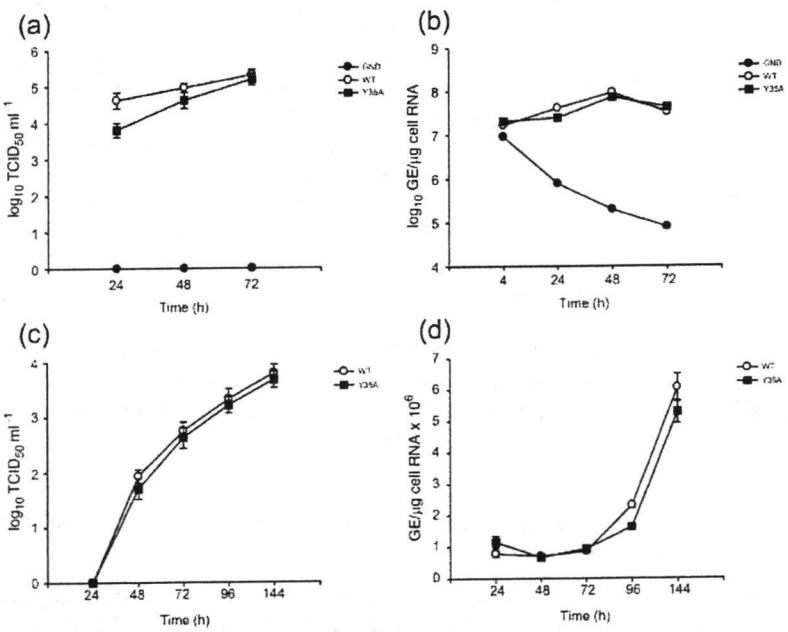

Fig. 6. Analysis of the core mutant viruses. (a, b) Determination of virus yield and intracellular RNA levels following transfection. HuH-7 cells were electroporated with RNA derived from $JFH1_{WT}$, $JFH1_{Y35A}$ or $JFH1_{GND}$ cDNA. At the indicated time points (a) the released virus titres and (b) the intracellular HCV RNA levels were quantified by $TCID_{50}$ and RT-qPCR, respectively. (c and d) Determination of virus yield and intracellular RNA levels following infection. Naïve HuH-7 cells were infected with $JFH1_{WT}$ or $JFH1_{Y35A}$ (obtained from the electroporated cells above) at an m.o.i. of 0.02. The (c) titres of infectious virus released into the medium and (d) intracellular viral RNA levels were measured over 6 days as described above. Means and error ranges from duplicate electroporations and infections are shown.

cells that had undergone efficient siRNA knockdown of DDX3 (Fig. 7a). As previously described, DDX3 knockdown cells were substantially less permissive for virus replication than normal cells following infection with $JFH1_{WT}$. Similar reductions in $JFH1_{Y35A}$ replication levels were also observed (Fig. 7b). Collectively, the data presented in Figs 6 and 7 indicate that DDX3 promotes efficient HCV infection by processes that are independent of its interaction with the viral core protein.

DISCUSSION

The recent advent of the HCV cell culture system has enabled us to further characterize the core–DDX3 interaction in the context of the complete HCV life cycle. Our overall goal is to deduce the role of DDX3 in normal cells with a view to understanding the significance of its interaction with HCV core in the virus life cycle and pathogenesis. Towards this end, we generated a large panel of mAbs recognizing different regions of DDX3. Using a subset of these, we confirmed that this interaction is genuine in JFH1-infected cells.

Given the putative function of DDX3 in RNA metabolism, initial identification of the core–DDX3 interaction led us and others to postulate its possible role in virus replication and assembly (Mamiya & Worman, 1999; Owsianka & Patel, 1999; You *et al.*, 1999). Recent data using the JFH1 system suggest that HCV RNA replication and virus assembly occur in LD-associated membranes (Boulant *et al.*, 2007; Miyanari *et al.*, 2007). Core protein, which associates with LDs (McLauchlan, 2000; Roingeard & Hourioux, 2008), recruits the viral non-structural proteins, replication complexes and envelope glycoproteins to these sites, allowing virus assembly to proceed in this local environment (Miyanari *et al.*, 2007). We show here that core also recruits the cellular DDX3 to LDs, suggesting that it may have a function in HCV replication. In keeping with this, two recent studies have shown reductions in JFH1 replication when DDX3 is removed from the cell by siRNA (Ariumi *et al.*, 2007; Randall *et al.*, 2007). We hypothesized that disrupting the association between HCV core and DDX3 might be detrimental to HCV replication, and provide insights into the purpose of this interaction. Our mutagenesis analysis revealed that the Y35A substitution in the JFH1 core molecule abrogated this interaction without affecting core–LD association. No alteration to virus RNA replication, translation or infectious particle production was observed following transfection of this mutant viral RNA into the cells. Similarly, $JFH1_{Y35A}$ virus yields from cells infected with the mutant progeny were equivalent to those of the WT virus. Interestingly, the two other mutants identified in this study ($JFH1_{F24A}$ and $JFH1_{G27A}$) showed greater reductions in virus replication, particularly post-infection (Supplementary Fig. S3, available in JGV Online). However, given their interaction with DDX3 is only slightly reduced (Fig. 5), this impairment is unlikely to be related to the disruption of the core–DDX3 interaction. A more plausible explanation for their unusual phenotypes could be an alteration in core function and/or RNA structure resulting from an alanine substitution at these positions, and as such these mutants require further investigations. Nevertheless, our results collectively suggest that the core–DDX3 interaction plays no role in virus morphogenesis.

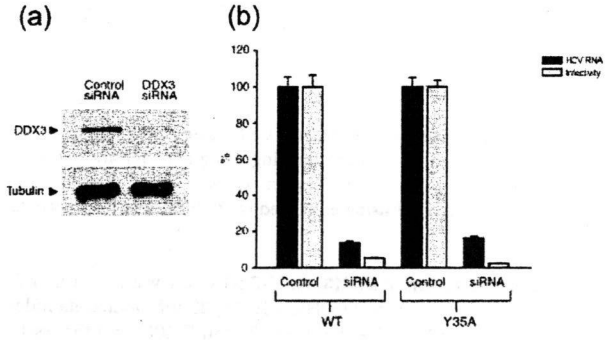

Fig. 7. Infection of DDX3 knockdown cells. (a) HuH-7 cells were transfected with siRNA duplexes as indicated. Cells were harvested after 2 days and examined by Western blotting using the anti-DDX3 mAb AO196. (b) Naïve and DDX3-deficient HuH-7 cells were infected with WT $JFH1_{WT}$ or $JFH1_{Y35A}$ virus. At 2 days post-infection the levels of released virus and intracellular HCV RNA were measured by $TCID_{50}$ assay and RT-qPCR, respectively. Means and error ranges from duplicate infections are shown.

Subgenomic replicons that do not possess core replicate as well as, if not better than, replicons encoding the entire polyprotein (Blight *et al.*, 2000; Ikeda *et al.*, 2002; Lohmann *et al.*, 1999), which indicates that the core–DDX3 interaction per se is not essential for HCV RNA replication. Nevertheless, Ariumi *et al.* (2007) reported that subgenomic replicons showed a twofold decrease in RNA replication in DDX3 knockdown cells. This finding raises an intriguing prospect that DDX3 may play a direct role in HCV RNA replication independent of and in addition to its interaction with core. Nonetheless, these workers observed a much greater reduction in JFH1 RNA replication in cells supporting replication of full genome-length RNAs, indicating greater importance of DDX3 in this setting and supporting the functional relevance of the interaction of DDX3 with core. We reproduced the deleterious effects of DDX3 knockdown on the $JFH1_{WT}$ replication but also found a similar phenotype for $JFH1_{Y35A}$ (Fig. 7). This finding further supports the notion of the core–DDX3 interaction having no function in HCV replication. Therefore, our data make a clear distinction between the effects of siRNA knockdown of DDX3 from the cells and disruption of the core–DDX3 interaction on HCV replication.

The possible involvement of the core–DDX3 interaction in pathogenesis cannot be discounted. Indeed, core protein has been widely implicated in modulating cellular functions, mainly due to its interaction with numerous host

factors (McLauchlan, 2000; Ray & Ray, 2001; Watashi & Shimotohno, 2003). Differential regulation of DDX3 has been reported in a number of tumours, including HCC, suggesting that it may be involved in HCV-associated pathogenesis (Botlagunta *et al.*, 2008; Chang *et al.*, 2006; Chao *et al.*, 2006; Huang *et al.*, 2004). DDX3 is also one of several DEAD-box proteins that are upregulated during HIV-1 replication (Krishnan & Zeichner, 2004). Interestingly, it is also upregulated during immune response to lipopolysaccharide-induced inflammation and during interferon treatment (de Veer *et al.*, 2001; Saban *et al.*, 2006). Thus, it is possible that during active viral replication HCV recruits DDX3 protein to evade host immune recognition, thereby adversely affecting one or more of its roles in normal cells (Rosner & Rinkevich, 2007) and in turn contributing to viral pathogenesis. Although we observed no differences in DDX3 expression levels between JFH1-infected cultured cells and uninfected cells, its relevance *in vivo* from a long-term disease perspective warrants further investigation.

METHODS

Cell culture and antibodies. Human hepatoma HuH-7 (Nakabayashi *et al.*, 1982) cells were propagated as described previously (Witteveldt *et al.*, 2009). The anti-NS5A mouse monoclonal antibody (mAb) 9E10 was a kind gift from Charles M. Rice (Center for the Study of Hepatitis C, The Rockefeller University, New York, USA) (Lindenbach *et al.*, 2005). The anti-HCV core rabbit serum R308, and the anti-ADRP sheep serum have been described previously (Hope & McLauchlan, 2000; Targett-Adams *et al.*, 2003). The anti-HCV core mAb c7-50 and the anti-α-tubulin and anti-GFP mAbs were purchased from Bioreagents and Sigma, respectively.

Generation and characterization of anti-DDX3 antibodies. BALB/c mice and rabbits were immunized with a bacterially expressed glutathione *S*-transferase-full-length DDX3 (GST–DDX3) fusion protein and antibodies generated essentially as previously described (Clayton *et al.*, 2002). A total of two rabbit polyclonal antisera (R647 and R648) and 16 mouse hybridomas secreting mAbs (see Fig. 1) to DDX3 was generated. The mAbs were initially identified and selected on the basis of their ability to interact with GST–DDX3, but not an irrelevant GST fusion protein, in an ELISA assay (data not shown).

Plasmid constructs and mutagenesis. The full-length DDX3 gene was cloned into the *Bam*HI site, in-frame to sequences encoding the EGFP, in the vector pEGFP-C1 (Clontech) to generate EGFP–DDX3 fusion protein.

To identify residues within the N-terminal 59 aa of HCV core that are critical for interaction with DDX3, EP-PCR was performed to introduce random mutations into the HCV genotype 1a strain H77c (Yanagi *et al.*, 1997) sequence encoding this region. The fidelity of *Taq* polymerase was decreased by altering the relative dNTP concentrations, using a high Mg^{2+} concentration and including Mn^{2+} in the reaction as described previously (Pritchard *et al.*, 2005). The mutated sequences were cloned in-frame with (and downstream of) green fluorescence protein (GFP) in the bacterial expression vector pKK223-3 (Pharmacia) and the library of core 1–59 mutant–GFP fusion proteins generated was screened in an *in vitro* DDX3-binding assay as described in Results. Nucleotide sequencing subsequently identified the mutations introduced by EP-PCR in the clones of interest.

The plasmid pUC-JFH1 carries the full-length cDNA of the genotype 2a HCV strain JFH1 (Wakita *et al.*, 2005). The plasmids pUC-GND JFH1 and pUC-JFH1 ΔE1E2 are identical except that they carry the GND mutation in the NS5B-encoding sequence, or an in-frame deletion in the E1 and E2 sequences (Wakita *et al.*, 2005). Site-directed mutagenesis was carried out using the QuikChange-II kit (Stratagene) to introduce alanine substitutions at the target sites in core. Briefly, various alanine substitutions in the core-coding region were individually introduced into the plasmid pGEM-T (Promega) carrying nt 1–2614 (corresponding to the 5′ UTR and core to E2 coding sequence) of HCV strain JFH1 using appropriate primers (the sequences of which are available upon request). The presence of the desired mutation in the resulting clones was confirmed by nucleotide sequencing. Sequences carrying the appropriate mutation were subcloned back into pJFH1-pUC to generate mutant viruses (see below).

Generation of JFH1 virus and its mutated derivatives. Ten micrograms of RNA synthesized *in vitro* using linearized plasmid templates carrying the wild-type (WT) or mutated JFH1 genomic cDNA was electroporated into HuH-7 cells as described previously (Wakita *et al.*, 2005). The electroporated cells were seeded into appropriate tissue culture dishes and incubated at 37 °C. At the indicated time period, the medium containing the infectious virus progeny was filtered through a 0.45 μm pore-sized membrane and infectivity determined as described below.

Determination of virus infectivity and RNA replication. Virus titres in the culture supernatants were determined as $TCID_{50}$ (Lindenbach *et al.*, 2005) following immunostaining for NS5A. The intracellular and extracellular HCV RNA content was measured by reverse transcription-quantitative real-time-polymerase chain reaction (RT-qPCR) as described previously (Witteveldt *et al.*, 2009). To determine virus replication after electroporation, cells transfected with the respective transcript were seeded into 10 cm culture dishes, incubated at 37 °C for 4 h and then trypsinized. Total RNA was prepared from 1/15 of the trypsinized cells using the RNeasy kit (Qiagen) to quantify viral RNA by qRT-PCR assay. The remaining cell suspension was split 1:3 into three T25 flasks. Following incubation at 37 °C for 24, 48 and 72 h, the infectious virus yields in cell culture supernatants were determined by $TCID_{50}$ assay and the intracellular viral RNA levels quantified by RT-qPCR. To measure virus replication after infection, 5.3×10^3 naïve HuH-7 cells seeded into six-well culture dishes were infected with virus at the indicated m.o.i. Following incubation at 37 °C for 24, 48, 72, 96 and 144 h, infectious virus yields and intracellular viral RNA levels were determined as described above.

SDS-PAGE and Western blotting. Cell lysates were subjected to SDS-PAGE followed by Western blotting using appropriate antibodies as described previously (Clayton *et al.*, 2002). The bound antibodies were detected using enhanced chemiluminescence reagents (Amersham).

Immunoprecipitation of DDX3. HuH-7 cells were washed with PBS, lysed in lysis buffer (20 mM Tris/HCl pH 7.4, 20 mM iodoacetamide, 150 mM NaCl, 1 mM EDTA and 0.5 % Triton X-100) and the lysate was spun briefly to remove nuclei. The clarified cell lysates were incubated with the anti-DDX3 antibodies as described in the text and the immune complexes precipitated using protein G agarose beads (Sigma). Following washes of the Sepharose beads, the immune complexes were analysed by SDS-PAGE followed by Western blotting using biotinylated R648 and anti-streptavidin-horseradish peroxidase (HRP) conjugate.

Co-immunoprecipitation of HCV core protein. Approximately, 5×10^6 HuH-7 cells electroporated with viral RNA were seeded into

100 mm tissue culture dishes. At 72 h post-transfection, the cells were washed and lysed in 0.5 ml lysis buffer (20 mM Tris/HCl, pH 7.4, 135 mM NaCl and 0.1 % Triton X-100) supplemented with 50 mM NAF, 5 mM Na_3VO_4 and 1 mM PMSF. The lysate was spun briefly to remove nuclei. After pre-clearing, the clarified lysate was immunoprecipitated overnight with protein G agarose beads that had been pre-incubated with the anti-DDX3 antiserum R648. The beads carrying the immune complex were spun at 2000 r.p.m. (microcentrifuge) for 2 min, washed three times with the lysis buffer and subjected to non-reducing SDS-PAGE followed by Western blotting using the anti-core mAb c7-50 and anti-mouse IgG-HRP conjugate.

Indirect immunofluorescence. Cells on coverslips were fixed in methanol and probed with the indicated primary antibody for 1 h at room temperature. After washing with PBS, cells were incubated with anti-species antibodies conjugated with fluorescein isothiocyanate, tetramethyl rhodamine isothiocyanate or Cy5 (Invitrogen) for 1 h and then washed with PBS. The coverslips were examined with a Zeiss Laser Scanning LSM510 META inverted confocal microscope (Carl Zeiss) and the images analysed using LSM510 software. Three-dimensional (3D) reconstructions were performed from Z-stack images collected using optimum intervals. Image stacks were deconvolved by 3D-blind deconvolution using Autodeblur software (MediaCybernetics), and 3D reconstructions were generated as described previously (Boulant *et al.*, 2007; Targett-Adams *et al.*, 2008).

RNA interference. Two pre-validated siRNA duplexes (s4004 and s4005, synthesized by Applied Biosystems) targeting different regions of the human DDX3 and a negative control siRNA composed of a scrambled sequence were used. Naïve HuH-7 cells plated overnight were transfected with lipofectamine RNAiMax (Invitrogen) and 50 nM siRNAs according to the manufacturer's protocol. The cells were then incubated for a further 2 days prior to virus infection. The efficiency of DDX3 knockdown was determined by immunoblotting using mAb AO196.

ACKNOWLEDGEMENTS

We thank Duncan McGeoch for helpful criticism of this manuscript and Charles M. Rice for the anti-NS5A mAb 9E10. This work was funded in part by grants from the Medical Research Council, UK (A. H. P.), Marie Curie Intra-European Fellowship contract 025198 (S. B.), the National Institute of Allergy and Infectious Diseases, U19-AI40035 (S. M. L.) and by the National Institute of Health, AI069285 (K. L.).

REFERENCES

Ariumi, Y., Kuroki, M., Abe, K., Dansako, H., Ikeda, M., Wakita, T. & Kato, N. (2007). DDX3 DEAD-box RNA helicase is required for hepatitis C virus RNA replication. *J Virol* **81**, 13922–13926.

Barba, G., Harper, F., Harada, T., Kohara, M., Goulinet, S., Matsuura, Y., Eder, G., Schaff, Z., Chapman, M. J. & other authors (1997). Hepatitis C virus core protein shows a cytoplasmic localization and associates to cellular lipid storage droplets. *Proc Natl Acad Sci U S A* **94**, 1200–1205.

Beckham, C., Hilliker, A., Cziko, A. M., Noueiry, A., Ramaswami, M. & Parker, R. (2008). The DEAD-Box RNA helicase Ded1p affects and accumulates in *Saccharomyces cerevisiae* P-bodies. *Mol Biol Cell* **19**, 984–993.

Blight, K. J., Kolykhalov, A. A. & Rice, C. M. (2000). Efficient initiation of HCV RNA replication in cell culture. *Science* **290**, 1972–1974.

Botlagunta, M., Vesuna, F., Mironchik, Y., Raman, A., Lisok, A., Winnard, P., Jr, Mukadam, S., Van Diest, P., Chen, J. H. & other authors (2008). Oncogenic role of DDX3 in breast cancer biogenesis. *Oncogene* **27**, 3912–3922.

Boulant, S., Vanbelle, C., Ebel, C., Penin, F. & Lavergne, J. P. (2005). Hepatitis C virus core protein is a dimeric alpha-helical protein exhibiting membrane protein features. *J Virol* **79**, 11353–11365.

Boulant, S., Montserret, R., Hope, R. G., Ratinier, M., Targett-Adams, P., Lavergne, J. P., Penin, F. & McLauchlan, J. (2006). Structural determinants that target the hepatitis C virus core protein to lipid droplets. *J Biol Chem* **281**, 22236–22247.

Boulant, S., Targett-Adams, P. & McLauchlan, J. (2007). Disrupting the association of hepatitis C virus core protein with lipid droplets correlates with a loss in production of infectious virus. *J Gen Virol* **88**, 2204–2213.

Bukh, J., Miller, R. H. & Purcell, R. H. (1995). Genetic heterogeneity of hepatitis C virus: quasispecies and genotypes. *Semin Liver Dis* **15**, 41–63.

Chang, P. C., Chi, C. W., Chau, G. Y., Li, F. Y., Tsai, Y. H., Wu, J. C. & Wu Lee, Y. H. (2006). DDX3, a DEAD box RNA helicase, is deregulated in hepatitis virus-associated hepatocellular carcinoma and is involved in cell growth control. *Oncogene* **25**, 1991–2003.

Chao, C. H., Chen, C. M., Cheng, P. L., Shih, J. W., Tsou, A. P. & Lee, Y. H. (2006). DDX3, a DEAD box RNA helicase with tumor growth-suppressive property and transcriptional regulation activity of the p21waf1/cip1 promoter, is a candidate tumor suppressor. *Cancer Res* **66**, 6579–6588.

Chen, S. L. & Morgan, T. R. (2006). The natural history of hepatitis C virus (HCV) infection. *Int J Med Sci* **3**, 47–52.

Clayton, R. F., Owsianka, A., Aitken, J., Graham, S., Bhella, D. & Patel, A. H. (2002). Analysis of antigenicity and topology of E2 glycoprotein present on recombinant hepatitis C virus-like particles. *J Virol* **76**, 7672–7682.

Cordin, O., Banroques, J., Tanner, N. K. & Linder, P. (2006). The DEAD-box protein family of RNA helicases. *Gene* **367**, 17–37.

Deckert, J., Hartmuth, K., Boehringer, D., Behzadnia, N., Will, C. L., Kastner, B., Stark, H., Urlaub, H. & Luhrmann, R. (2006). Protein composition and electron microscopy structure of affinity-purified human spliceosomal B complexes isolated under physiological conditions. *Mol Cell Biol* **26**, 5528–5543.

de Veer, M. J., Holko, M., Frevel, M., Walker, E., Der, S., Paranjape, J. M., Silverman, R. H. & Williams, B. R. (2001). Functional classification of interferon-stimulated genes identified using microarrays. *J Leukoc Biol* **69**, 912–920.

Franca, R., Belfiore, A., Spadari, S. & Maga, G. (2007). Human DEAD-box ATPase DDX3 shows a relaxed nucleoside substrate specificity. *Proteins* **67**, 1128–1137.

Fujimoto, Y., Itabe, H., Sakai, J., Makita, M., Noda, J., Mori, M., Higashi, Y., Kojima, S. & Takano, T. (2004). Identification of major proteins in the lipid droplet-enriched fraction isolated from the human hepatocyte cell line HuH7. *Biochim Biophys Acta* **1644**, 47–59.

Gururajan, R., Perry-O'Keefe, H., Melton, D. A. & Weeks, D. L. (1991). The *Xenopus* localized messenger RNA An3 may encode an ATP-dependent RNA helicase. *Nature* **349**, 717–719.

Hope, R. G. & McLauchlan, J. (2000). Sequence motifs required for lipid droplet association and protein stability are unique to the hepatitis C virus core protein. *J Gen Virol* **81**, 1913–1925.

Huang, J. S., Chao, C. C., Su, T. L., Yeh, S. H., Chen, D. S., Chen, C. T., Chen, P. J. & Jou, Y. S. (2004). Diverse cellular transformation capability of overexpressed genes in human hepatocellular carcinoma. *Biochem Biophys Res Commun* **315**, 950–958.

Ikeda, M., Yi, M., Li, K. & Lemon, S. M. (2002). Selectable subgenomic and genome-length dicistronic RNAs derived from an infectious molecular clone of the HCV-N strain of hepatitis C virus replicate efficiently in cultured Huh7 cells. *J Virol* **76**, 2997–3006.

Jamieson, D. J. & Beggs, J. D. (1991). A suppressor of yeast spp81/ded1 mutations encodes a very similar putative ATP-dependent RNA helicase. *Mol Microbiol* **5**, 805–812.

Kanai, Y., Dohmae, N. & Hirokawa, N. (2004). Kinesin transports RNA: isolation and characterization of an RNA-transporting granule. *Neuron* **43**, 513–525.

Krishnan, V. & Zeichner, S. L. (2004). Alterations in the expression of DEAD-box and other RNA binding proteins during HIV-1 replication. *Retrovirology* **1**, 42.

Leroy, P., Alzari, P., Sassoon, D., Wolgemuth, D. & Fellous, M. (1989). The protein encoded by a murine male germ cell-specific transcript is a putative ATP-dependent RNA helicase. *Cell* **57**, 549–559.

Lindenbach, B. D., Evans, M. J., Syder, A. J., Wolk, B., Tellinghuisen, T. L., Liu, C. C., Maruyama, T., Hynes, R. O., Burton, D. R. & other authors (2005). Complete replication of hepatitis C virus in cell culture. *Science* **309**, 623–626.

Lohmann, V., Korner, F., Koch, J., Herian, U., Theilmann, L. & Bartenschlager, R. (1999). Replication of subgenomic hepatitis C virus RNAs in a hepatoma cell line. *Science* **285**, 110–113.

Mamiya, N. & Worman, H. J. (1999). Hepatitis C virus core protein binds to a DEAD box RNA helicase. *J Biol Chem* **274**, 15751–15756.

McLauchlan, J. (2000). Properties of the hepatitis C virus core protein: a structural protein that modulates cellular processes. *J Viral Hepat* **7**, 2–14.

Miyanari, Y., Atsuzawa, K., Usuda, N., Watashi, K., Hishiki, T., Zayas, M., Bartenschlager, R., Wakita, T., Hijikata, M. & Shimotohno, K. (2007). The lipid droplet is an important organelle for hepatitis C virus production. *Nat Cell Biol* **9**, 1089–1097.

Moradpour, D., Wakita, T., Tokushige, K., Carlson, R. I., Krawczynski, K. & Wands, J. R. (1996). Characterization of three novel monoclonal antibodies against hepatitis C virus core protein. *J Med Virol* **48**, 234–241.

Moradpour, D., Penin, F. & Rice, C. M. (2007). Replication of hepatitis C virus. *Nat Rev Microbiol* **5**, 453–463.

Nakabayashi, H., Taketa, K., Miyano, K., Yamane, T. & Sato, J. (1982). Growth of human hepatoma cells lines with differentiated functions in chemically defined medium. *Cancer Res* **42**, 3858–3863.

Noueiry, A. O., Chen, J. & Ahlquist, P. (2000). A mutant allele of essential, general translation initiation factor DED1 selectively inhibits translation of a viral mRNA. *Proc Natl Acad Sci U S A* **97**, 12985–12990.

Owsianka, A. M. & Patel, A. H. (1999). Hepatitis C virus core protein interacts with a human DEAD box protein DDX3. *Virology* **257**, 330–340.

Pawlotsky, J. M. (2003). Hepatitis C virus genetic variability: pathogenic and clinical implications. *Clin Liver Dis* **7**, 45–66.

Pritchard, L., Corne, D., Kell, D., Rowland, J. & Winson, M. (2005). A general model of error-prone PCR. *J Theor Biol* **234**, 497–509.

Randall, G., Panis, M., Cooper, J. D., Tellinghuisen, T. L., Sukhodolets, K. E., Pfeffer, S., Landthaler, M., Landgraf, P., Kan, S. & other authors (2007). Cellular cofactors affecting hepatitis C virus infection and replication. *Proc Natl Acad Sci U S A* **104**, 12884–12889.

Ray, R. B. & Ray, R. (2001). Hepatitis C virus core protein: intriguing properties and functional relevance. *FEMS Microbiol Lett* **202**, 149–156.

Rocak, S. & Linder, P. (2004). DEAD-box proteins: the driving forces behind RNA metabolism. *Nat Rev Mol Cell Biol* **5**, 232–241.

Roingeard, P. & Hourioux, C. (2008). Hepatitis C virus core protein, lipid droplets and steatosis. *J Viral Hepat* **15**, 157–164.

Rosner, A. & Rinkevich, B. (2007). The DDX3 subfamily of the DEAD box helicases: divergent roles as unveiled by studying different organisms and in vitro assays. *Curr Med Chem* **14**, 2517–2525.

Saban, M. R., Hellmich, H. L., Turner, M., Nguyen, N. B., Vadigepalli, R., Dyer, D. W., Hurst, R. E., Centola, M. & Saban, R. (2006). The inflammatory and normal transcriptome of mouse bladder detrusor and mucosa. *BMC Physiol* **6**, 1.

Sato, S., Fukasawa, M., Yamakawa, Y., Natsume, T., Suzuki, T., Shoji, I., Aizaki, H., Miyamura, T. & Nishijima, M. (2006). Proteomic profiling of lipid droplet proteins in hepatoma cell lines expressing hepatitis C virus core protein. *J Biochem* **139**, 921–930.

Schroder, M., Baran, M. & Bowie, A. G. (2008). Viral targeting of DEAD box protein 3 reveals its role in TBK1/IKKε-mediated IRF activation. *EMBO J* **27**, 2147–2157.

Sekiguchi, T., Kurihara, Y. & Fukumura, J. (2007). Phosphorylation of threonine 204 of DEAD-box RNA helicase DDX3 by cyclin B/cdc2 in vitro. *Biochem Biophys Res Commun* **356**, 668–673.

Shavinskaya, A., Boulant, S., Penin, F., McLauchlan, J. & Bartenschlager, R. (2007). The lipid droplet binding domain of hepatitis C virus core protein is a major determinant for efficient virus assembly. *J Biol Chem* **282**, 37158–37169.

Shih, J. W., Tsai, T. Y., Chao, C. H. & Wu Lee, Y. H. (2008). Candidate tumor suppressor DDX3 RNA helicase specifically represses cap-dependent translation by acting as an eIF4E inhibitory protein. *Oncogene* **27**, 700–714.

Simmonds, P. (1995). Variability of hepatitis C virus. *Hepatology* **21**, 570–583.

Soulat, D., Burckstummer, T., Westermayer, S., Goncalves, A., Bauch, A., Stefanovic, A., Hantschel, O., Bennett, K. L., Decker, T. & Superti-Furga, G. (2008). The DEAD-box helicase DDX3X is a critical component of the TANK-binding kinase 1-dependent innate immune response. *EMBO J* **27**, 2135–2146.

Sun, M., Song, L., Li, Y., Zhou, T. & Jope, R. S. (2008). Identification of an antiapoptotic protein complex at death receptors. *Cell Death Differ* **15**, 1887–1900.

Targett-Adams, P., Chambers, D., Gledhill, S., Hope, R. G., Coy, J. F., Girod, A. & McLauchlan, J. (2003). Live cell analysis and targeting of the lipid droplet-binding adipocyte differentiation-related protein. *J Biol Chem* **278**, 15998–16007.

Targett-Adams, P., Boulant, S. & McLauchlan, J. (2008). Visualization of double-stranded RNA in cells supporting hepatitis C virus RNA replication. *J Virol* **82**, 2182–2195.

Wakita, T., Pietschmann, T., Kato, T., Date, T., Miyamoto, M., Zhao, Z., Murthy, K., Habermann, A., Krausslich, H. G. & other authors (2005). Production of infectious hepatitis C virus in tissue culture from a cloned viral genome. *Nat Med* **11**, 791–796.

Wang, H., Kim, S. & Ryu, W. S. (2009). DDX3 DEAD-Box RNA helicase inhibits hepatitis B virus reverse transcription by incorporation into nucleocapsids. *J Virol* **83**, 5815–5824.

Watashi, K. & Shimotohno, K. (2003). The roles of hepatitis C virus proteins in modulation of cellular functions: a novel action mechanism of the HCV core protein on gene regulation by nuclear hormone receptors. *Cancer Sci* **94**, 937–943.

Witteveldt, J., Evans, M. J., Bitzegeio, J., Koutsoudakis, G., Owsianka, A. M., Angus, A. G., Keck, Z. Y., Foung, S. K., Pietschmann, T. & other authors (2009). CD81 is dispensable for

hepatitis C virus cell-to-cell transmission in hepatoma cells. *J Gen Virol* **90**, 48–58.

Yanagi, M., Purcell, R. H., Emerson, S. U. & Bukh, J. (1997). Transcripts from a single full-length cDNA clone of hepatitis C virus are infectious when directly transfected into the liver of a chimpanzee. *Proc Natl Acad Sci U S A* **94**, 8738–8743.

Yedavalli, V. S., Neuveut, C., Chi, Y. H., Kleiman, L. & Jeang, K. T. (2004). Requirement of DDX3 DEAD box RNA helicase for HIV-1 Rev-RRE export function. *Cell* **119**, 381–392.

Yi, M., Ma, Y., Yates, J. & Lemon, S. M. (2007). Compensatory mutations in E1, p7, NS2, and NS3 enhance yields of cell culture-infectious intergenotypic chimeric hepatitis C virus. *J Virol* **81**, 629–638.

You, L. R., Chen, C. M., Yeh, T. S., Tsai, T. Y., Mai, R. T., Lin, C. H. & Lee, Y. H. (1999). Hepatitis C virus core protein interacts with cellular putative RNA helicase. *J Virol* **73**, 2841–2853.

Zhou, Z., Licklider, L. J., Gygi, S. P. & Reed, R. (2002). Comprehensive proteomic analysis of the human spliceosome. *Nature* **419**, 182–185.

JOURNAL OF VIROLOGY, May 2009, p. 5137–5147 Vol. 83, No. 10
0022-538X/09/$08.00+0 doi:10.1128/JVI.02179-08

Involvement of Creatine Kinase B in Hepatitis C Virus Genome Replication through Interaction with the Viral NS4A Protein▽

Hiromichi Hara,[1,2] Hideki Aizaki,[1] Mami Matsuda,[1] Fumiko Shinkai-Ouchi,[3] Yasushi Inoue,[1,4] Kyoko Murakami,[1] Ikuo Shoji,[1,5] Hayato Kawakami,[6] Yoshiharu Matsuura,[7] Michael M. C. Lai,[8] Tatsuo Miyamura,[1] Takaji Wakita,[1] and Tetsuro Suzuki[1]*

Department of Virology II[1] and Department of Biochemistry and Cell Biology,[3] National Institute of Infectious Diseases, Tokyo 162-8640, Japan; Department of Internal medicine, Division of Pulmonary Diseases, The Jikei University School of Medicine, Tokyo 105-8461, Japan[2]; Mita Hospital, International University of Health and Welfare, Tokyo 108-8329, Japan[4]; Division of Microbiology, Kobe University Graduate School of Medicine, Hyogo 650-0017, Japan[5]; Department of Anatomy, Kyorin University School of Medicine, Tokyo 181-8611, Japan[6]; Research Institute for Microbial Diseases, Osaka University, Osaka 565-0871, Japan[7]; and Department of Molecular Microbiology and Immunology, University of Southern California, Keck School of Medicine, Los Angeles, California 90033[8]

Received 15 October 2008/Accepted 20 February 2009

Persistent infection with hepatitis C virus (HCV) is a major cause of chronic liver diseases. The aim of this study was to identify host cell factor(s) participating in the HCV replication complex (RC) and to clarify the regulatory mechanisms of viral genome replication dependent on the host-derived factor(s) identified. By comparative proteome analysis of RC-rich membrane fractions and subsequent gene silencing mediated by RNA interference, we identified several candidates for RC components involved in HCV replication. We found that one of these candidates, creatine kinase B (CKB), a key ATP-generating enzyme that regulates ATP in subcellular compartments of nonmuscle cells, is important for efficient replication of the HCV genome and propagation of infectious virus. CKB interacts with HCV NS4A protein and forms a complex with NS3-4A, which possesses multiple enzyme activities. CKB upregulates both NS3-4A-mediated unwinding of RNA and DNA in vitro and replicase activity in permeabilized HCV replicating cells. Our results support a model in which recruitment of CKB to the HCV RC compartment, which has high and fluctuating energy demands, through its interaction with NS4A is important for efficient replication of the viral genome. The CKB-NS4A association is a potential target for the development of a new type of antiviral therapeutic strategy.

Hepatitis C virus (HCV) infection represents a significant global healthcare burden, and current estimates suggest that a minimum of 3% of the world's population is chronically infected (4, 19). The virus is responsible for many cases of severe chronic liver diseases, including cirrhosis and hepatocellular carcinoma (4, 16, 19). HCV is a positive-stranded RNA virus belonging to the family *Flaviviridae*. Its ~9.6-kb genome is translated into a single polypeptide of about 3,000 amino acids (aa), in which the nonstructural (NS) proteins NS2, NS3, NS4A, NS4B, NS5A, and NS5B reside in the C-terminal half region (6, 34, 44). NS4A, a small 7-kDa protein, functions as a cofactor for NS3 to enhance NS3 enzyme activities such as serine protease and helicase activities. The hydrophobic N-terminal region of NS4A, which is predicted to form a transmembrane α-helix, is responsible for membrane anchorage of the NS3-4A complex (8, 44, 50), and the central region of NS4A is important for the interaction with NS3 (10, 44). A recent study demonstrated the involvement of the C terminus of NS4A in the regulation of NS5A hyperphosphorylation and viral replication (28).

The development of HCV replicon technology several years ago accelerated research on viral RNA replication (7, 44). Furthermore, a robust cell culture system for propagation of infectious HCV particles was developed using a viral genome of HCV genotype 2a, JFH-1 strain, enabling us to study every process in the viral life cycle (27, 47, 54). RNA derived from genotype 1a, HCV H77, containing cell-culture adaptive mutations, also produces infectious viruses (52). Using these systems, it has been reported that the HCV genome replicates in a distinct, subcellular replication complex (RC) compartment, which includes NS3-5B and the viral RNA (2, 14, 33). The RC forms in a distinct compartment with high concentrations of viral and cellular components located on detergent-resistant membrane (DRM) structures, possibly a lipid-raft structure (2, 41), which may protect the RC from external proteases and nucleases. Almost all processes in viral replication are dependent on the host cell's machinery and involve intimate interaction between viral and host proteins. However, the functional roles of host factors interacting with the HCV RC in viral genome replication remain ambiguous.

To gain a better understanding of cellular factors that are components of the HCV RC and that function as regulators of viral replication, a comparative proteomic analysis of DRM fractions from HCV replicon and parental cells and subsequent RNA interference (RNAi) silencing of selected genes were performed. We identified creatine kinase B (CKB) as a key factor for the HCV genome replication. CKB catalyzes the reversible transfer of the phosphate group of phosphocreatine

* Corresponding author. Mailing address: Department of Virology II, National Institute of Infectious Diseases, 1-23-1 Toyama, Shinjuku-ku, Tokyo 162-8640, Japan. Phone: 81-3-5285-1111. Fax: 81-3-5285-1161. E-mail: tesuzuki@nih.go.jp.

▽ Published ahead of print on 4 March 2009.

(pCr) to ADP to yield ATP and creatine and is known to play important roles in local delivery and cellular compartmentalization of ATP (48, 51). The findings obtained here suggest that recruitment of CKB to the HCV RC, through CKB interaction with NS4A, is essential for maintenance or enhancement of viral replicase activity.

MATERIALS AND METHODS

Cell lines, antibodies, and reagents. Human hepatoma cell line Huh-7.5.1 (54) was kindly provided by Francis V. Chisari. Cell lines carrying subgenomic replicon RNAs, namely, SGR-N (41) and SGR-JFH1 (23), were derived from the HCV-N (17) and JFH-1 strains (24), respectively. Mouse monoclonal antibodies (MAbs) against HCV NS3 (Chemicon, Temecula, CA), NS4A (Santa Cruz Biotechnology, Inc., Santa Cruz, CA), NS5A (Biodesign, Saco, ME), NS5B (2), FLAG (M2; Sigma-Aldrich, St. Louis, MO), glyceraldehyde-3-phosphate dehydrogenase (GAPDH; Chemicon), and Flotillin-1 (BD Biosciences, San Jose, CA) and polyclonal antibodies (PAbs) against CKB (mouse [Abnova, Taipei, Taiwan], goat [Santa Cruz]), hemagglutinin (HA; Sigma-Aldrich), and FLAG (Sigma-Aldrich) were used. Cyclocreatine (Ccr; also known as 2-imino-1-imidazolidineacetic acid), pCr, and phosphopyruvic acid (pPy) were purchased from Sigma-Aldrich. Recombinant CKB and pyruvate kinase (PK) were obtained from Acris (Herfold, Germany) and Calbiochem (San Diego, CA), respectively.

Proteome analysis. RC-rich membrane fractions of cells were isolated as described previously (2, 41). Briefly, cells were lysed in hypotonic buffer. After removing the nuclei, supernatants were treated with 1% NP-40 for 60 min, mixed with 70% sucrose, overlaid with 55 and 10% sucrose, and centrifuged at 38,000 rpm for 14 h. Proteins from membrane fractions were purified by using a 2D Clean-Up kit (GE Healthcare, Tokyo, Japan), followed by labeling with fluorescent dyes: Cy5 for replicon cells, Cy3 for parental cells, and Cy2 for the protein standard containing equal amounts of both cell samples. Two-dimensional fluorescence difference gel electrophoresis (2D-DIGE) was performed using Immobiline DryStrip as the first-dimension gel and 12.5% polyacrylamide gel as the second-dimension gel. The 2D-DIGE images were analyzed quantitatively using the DeCyder software (GE Healthcare). Student *t* test was performed on differences between the tested samples using DeCyder biological variation analysis module. Samples were analyzed in triplicate. The protein spots of interest were excised from the gel, subjected to in-gel digestion using trypsin or lysyl endopeptidase and analyzed by liquid chromatography (MAGIC 2002 System; Michrom Bioresources, Auburn, CA) directly connected to electrospray ionization-ion trap mass spectrometry (LCQ-decaXP; Thermo Electron Corp., Iwakura, Japan). The results were subjected to database (NCBInr) search by Mascot server software (Matrix Science, Boston, MA) for peptide assignment.

Plasmids. A human CKB cDNA (43; kindly provided by Oriental Yeast Corp., Tokyo, Japan) was inserted into the EcoRI site of pCAGGS, yielding pCAGCKB. To generate expression plasmids for HA-tagged versions of wild-type and deletion mutated CKB, the corresponding DNA fragments were amplified by PCR, followed by introduction into the BglII site of pCAGGS. A fragment representing the inactive mutant CKB-C283S was synthesized by PCR mutagenesis. To generate FLAG-tagged NS protein expression plasmids, DNA fragments encoding either NS3, NS4A, NS4B, NS5A, or NS5B protein were amplified from HCV strains NIHJ1 (1) and JFH-1 (23) by PCR, followed by cloning into the EcoRI-EcoRV sites of pcDNA3-MEF (20). To generate an HA-tagged NS3 expression plasmid, a fragment encoding NS3 with the HA tag sequence at its N terminus was inserted into pCAGGS.

siRNA transfection. The small interfering RNAs (siRNAs) targeted to CKB (CKB-1 [5′-UAAGACCUUCCUGGUGUGGTT-3′] and CKB-2 [5′-CGUCAC CCUUGGUAGAGUUTT-3′]) and the scramble negative control siRNA to CKB-2 (5′-GGCGUACUAGCUUAUUCGCTT-3′) were purchased from Sigma. Cells in a 24-well plate were transfected with siRNA using HiPerFect transfection reagent (Qiagen, Tokyo, Japan) according to the manufacturer's instructions. The siRNA sequences for the other genes used in the siRNA screening are available upon request.

HCV infection. Culture media from Huh-7 cells transfected with in vitro-transcribed RNA corresponding to the full-length JFH-1 (47) was collected, concentrated, and used for the infection assay (3).

Quantification of HCV core protein and RNA. To estimate the levels of HCV core protein, aliquots of culture supernatants or of cell lysates were assayed by using HCV Core enzyme-linked immunosorbent assay kits (5). Total RNA was isolated from harvested cells using TRIzol (Invitrogen, Carlsbad, CA). Copy numbers of the viral RNA were determined by reverse transcription-PCR (RT-PCR) (2, 36, 46).

Immunoprecipitation, immunoblot analysis, and immunofluorescence microscopy. The analyses, as well as DNA transfection, were performed essentially as previously described (42). Cells were lysed in immunoprecipitation lysis buffer (50 mM Tris-HCl [pH 7.6], 150 mM NaCl, 1% sodium deoxycholate, 1% NP-40, 0.1% sodium dodecyl sulfate, 1 mM dithiothreitol, 1 mM calcium acetate). For immunoprecipitation, supernatants of cell lysates were precipitated with anti-FLAG antibody and protein A-Sepharose Fast Flow beads (GE healthcare). For immunofluorescence microscopy, anti-CKB goat PAb and anti-NS4A MAb as primary antibodies and Alexa Fluor 555-conjugated donkey anti-goat immunoglobulin G (Invitrogen) and Alexa Fluor 488-conjugated rabbit anti-mouse immunoglobulin G (Invitrogen) as secondary antibodies were used and observed under an LSM 510 confocal microscope (Carl Zeiss, Oberkochen, Germany).

Immunoelectron microscopy. Postembedding immunostaining using the colloidal gold-labeling method was performed as described previously (38). Cells were fixed in 4% paraformaldehyde–1% glutaraldehyde at 4°C for 1 h. After dehydration through a graded series of ethanol, cells were embedded in LR White (London Resin Company, London, United Kingdom) and sectioned. After blocking, section grids were incubated with a mixture of anti-NS4A and anti-CKB antibodies at 4°C overnight, followed by treatment with a mixture of 18-nm colloidal gold-conjugated donkey anti-mouse immunoglobulin G and 12-nm colloidal gold-conjugated donkey anti-goat immunoglobulin G antibodies (Jackson Immunoresearch, West Grove, PA) at 4°C overnight. The sections were stained with uranyl acetate and observed under a transmission electron microscope.

Measurement of CK activity and cellular ATP level. Cells were lysed with passive lysis buffer (Promega, Madison, WI), and CK activities were measured based on Oliver methods (40), in which the activity of converting creatine phosphate and ADP to creatine and ATP was measured. ATP levels in cell lysates were measured by using a CellTiter-Glo luminescent cell viability assay (Promega).

RNA replication assays in permeabilized replicon cells and in vitro. The RNA synthesis assay using permeabilized replicon cells was based on a previously described method (33). Briefly, SGR-JFH1 cells were treated with 5 μg of actinomycin D/ml for 2 h, followed by permeabilization with 50 μg of digitonin/ml for 5 min. The resulting mix was incubated with 500 μM concentrations of ATP, GTP, and CTP; 10 μCi of UTP ([α-^{32}P]UTP); 50 μg of actinomycin D/ml; and 5 mM pCr with or without 20 U of CKB/ml for 4 h at 27°C. RNA was extracted by using TRIzol and analyzed by 1% formaldehyde agarose gel electrophoresis. The cell-free RNA replication assay was performed as described previously (2).

In vitro helicase assays. Helicase activity on double-stranded RNA (dsRNA) was investigated as described previously (11) with some modifications. The 5′ end of the release strand was labeled with [γ-^{32}P]ATP using T4 polynucleotide kinase (Ambion). The dsRNA substrate was obtained by annealing the labeled RNA with a template strand RNA at a molar ratio of 1:1. The helicase assay mixture contained 5 nM dsRNA, helicase enzyme (80 nM NS3 or NS3-4A [kindly provided by R. De Francesco]), 6 mM ATP, in the presence or absence of 20 U of CKB/ml in an assay buffer (25 mM MOPS-NaOH [pH 7.0], 2.5 mM dithiothreitol, 100 μg of bovine serum albumin/ml, 3 mM $MgCl_2$, 5 mM pCr, 2.5 U of RNase inhibitor/ml). After the helicase reaction, samples were electrophoresed in a native 8% polyacrylamide gel and autoradiographed.

To determine the effect of PK/pPy system on the helicase activity, PK and pPy were used instead of CKB and pCr. Helicase activity on dsDNA was measured based on homogeneous time-resolved fluorescence quenching using a Trupoint helicase assay kit (Perkin-Elmer, Waltham, MA) according to the manufacturer's instructions.

In vitro protease assay. In vitro HCV protease activity of NS3-4A or NS3 was analyzed by using a SensoLyteHCV protease assay kit (AnaSpec, San Jose, CA) according to the manufacturer's instructions.

RESULTS

Identification of host factors involved in HCV RNA replication by comparative proteomic analysis of DRM fractions and RNAi silencing. To identify host proteins involved in the HCV RC, proteome profiles of the RC-rich membrane fraction in Huh-7 cells harboring subgenomic replicon RNA derived from genotype 1b, N isolate (SGR-N) were compared to those of parental cells by 2D-DIGE. We confirmed that the DRM fraction obtained from SGR-N cells is functionally active in a

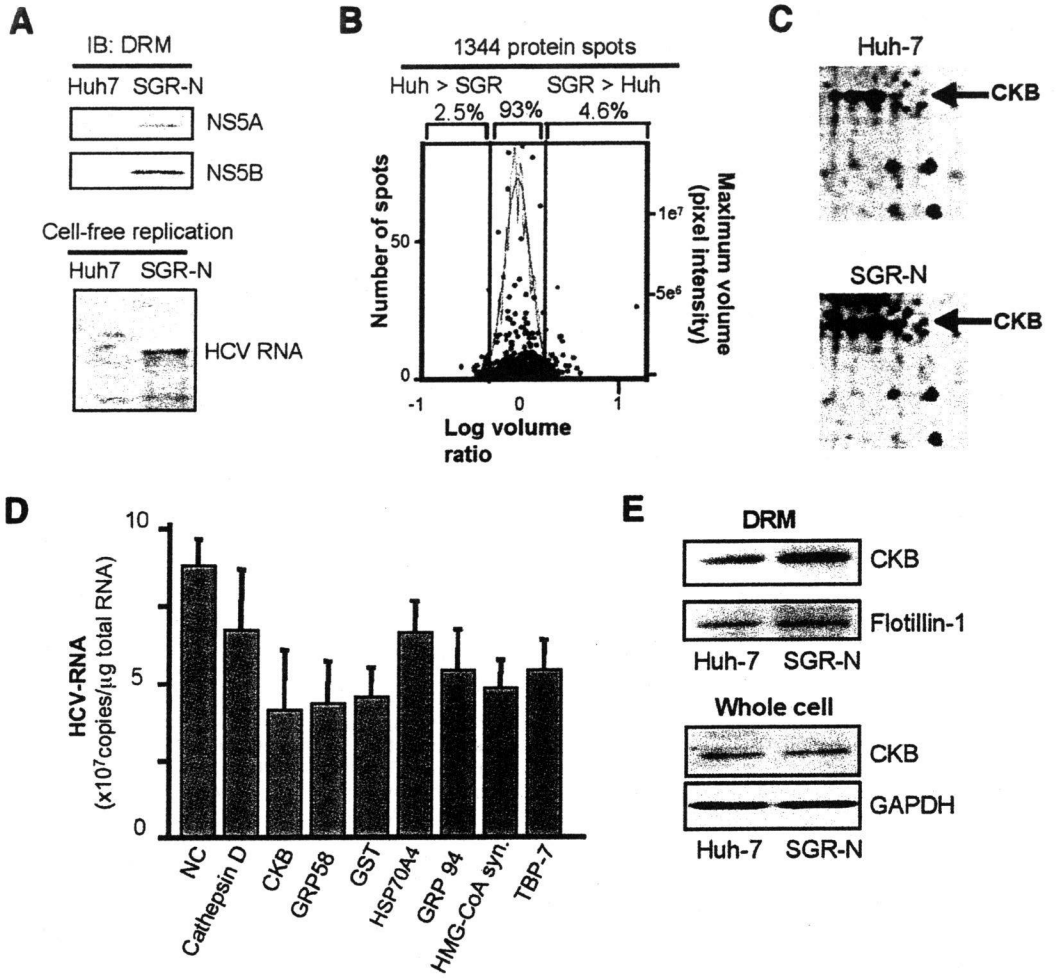

FIG. 1. Comparative proteomic analysis of DRM fractions and RNAi silencing. (A) Preparation of functionally active RC fraction for proteome analysis. DRM fractions obtained from SGR-N cells and parental Huh-7 cells were analyzed by immunoblotting with anti-NS5A and anti-NS5B antibodies (upper panel) and by the cell-free RNA replication assay (lower panel). (B) Histogram representation of proteins detected in 2D-DIGE. Images were analyzed quantitatively by the DeCyder software. The left and right *y* axis, respectively, indicate the spot frequency and the maximum volume of each spot, given against the log volume ratio (*x* axis). (C) Comparison of 2D-DIGE maps of proteins from DRM fractions of SGR-N cells and Huh-7 cells. Enlarged 2D-DIGE gel images of regions containing protein spots of CKB (arrows) are shown. (D) Effects of siRNAs of genes selected from comparative proteome analysis on HCV RNA replication. SGR-N cells were transfected with siRNA specific to cathepsin D, CKB (siCKB-1), GRP58, GST, Hsp70 protein 4, GRP94, HMG-coenzyme A synthase, or Tat binding protein 7 or with nontargeting (NC) siRNA. At 48 h posttransfection, total RNA was isolated and HCV RNA levels were assessed by real-time RT-PCR. (E) Enrichment of CKB in the DRM of HCV replicon cells. Equal amounts of DRM fractions from SGR-N and parental Huh-7 cells, or whole-cell lysates from both cells were analyzed by immunoblotting with antibodies against CKB, flotilin-1 or GAPDH.

cell-free replication assay (Fig. 1A). Three independent proteome experiments were performed for a reliable analysis of protein expression. Approximately 1,300 spots were resolved in each gel, and 4 to 5% of the protein spots represented a >2-fold increase in the membrane fraction of replicon cells in each experiment (Fig. 1B). The protein spots that exhibited high reproducibility (an example shown in Fig. 1C) were excised, digested by trypsin or lysyl endopeptidase, and analyzed by mass spectrometry, which identified the corresponding proteins in 27 cases (Table 1). Among the proteins implicated in a variety of functional categories, 10 were involved in protein folding, mainly as chaperones, 7 were metabolic and biosynthesis enzymes including proteins for redox regulation or energy pathways, 3 were involved in cytoskeleton organization, and 3 proteins were related to cellular processes, mainly proteolysis pathways. The viral NS proteins identified as differentially expressed proteins in the analysis were not listed.

In order to identify host factors involved in HCV replication, we examined the effects on viral RNA replication of transfection of SGR-N cells with siRNAs against genes encoding nine proteins belonging to diverse classes of biological functions (Table 1). Each siRNA reduced the HCV RNA level to 47 to 76% of the level of the siRNA control (Fig. 1D). None of the siRNAs tested exhibited considerable cytotoxicity against the replicon cells, ruling out overt toxicity as a mechanism for inhibition of viral RNA replication. Among the candidate

TABLE 1. Selected proteins that reproducibly increased in the DRM fraction of SGR-N cells[a]

Avg ratio	P (Student t test)	Coverage (%)	Protein name	Molecular function	GI no.
5.56	0.04	27	GRP94	Protein folding	15010550
4.99	0.07	47	Hsp60	Protein folding	6996447
3.73	0.07	6	tRNA guanine transglycosylase	Metabolism	30583205
3.56	0.06	23	KIAA0088	Unknown	577295
3.32	0.07	4	Thioredoxin-related protein	Unknown	20067392
3.32	0.13	12	Tat binding protein 1 (TBP-1)	Cellular processes	20532406
3.06	0.14	22	Aldehyde dehydrogenase 1	Metabolism	2183299
3.06	0.14	14	Chaperonin TRiC/CCT, subunit 2	Protein folding	54696794
2.96	0.04	14	Heat shock 70-kDa protein 4 (HSPA4)	Protein folding	6226869
2.96	0.04	29	GRP58	Metabolism/protein folding	2245365
2.94	0.01	37	Mutant β-actin	Cytoskeleton organization	28336
2.65	0.17	33	Glutathione S-transferase (GST)	Catalytic activity	2204207
2.53	0.04	37	Keratin 19	Cytoskeleton organization	6729681
2.46	0.08	6	Heterogeneous nuclear ribonucleoprotein K	Nucleic acid modification	460789
2.45	0.001	13	HMG-coenzyme A synthase	Metabolism	30009
2.4	0.02	31	CKB	Energy pathway/metabolism	180570
2.4	0.02	11	Cathepsin D	Cellular processes	30582659
2.4	0.02	11	C8orf2	Unknown	37181322
2.36	0.1	38	Tropomyosin 4-anaplastic lymphoma kinase fusion protein	Cytoskeleton organization	14010354
2.36	0.1	6	Calreticulin	Protein folding	30583735
2.33	0.01	29	Quinolinate phosphoribosyltransferase	Metabolism	30583301
2.29	0.04	25	Protein disulfide isomerase-related protein 5	Protein folding	1710248
2.29	0.04	16	Tat binding protein 7 (TBP-7)	Cellular processes	263099
2.05	0.11	24	Calumenin	Metabolism	2809324
2.05	0.12	10	TRiC/CCT, subunit 5	Protein folding	24307939
2.03	0.07	20	Hsp90 beta	Protein folding	34304590
2.01	0.07	10	TRiC/CCT, subunit 1	Protein folding	36796

[a] The spectra obtained by tandem mass spectrometry were collected using data-dependent mode, and the results were subjected to database (NCBInr) search by Mascot server software (Matrix Science, London, United Kingdom) for peptide assignment. Coverage, the ratio of the portion of protein sequence covered by matched peptides to the whole protein sequence. GI no., GenInfo identifier number.

genes examined, we observed a reproducible inhibition of HCV RNA replication by two independent siRNAs targeting CKB (see below).

CKB participates in HCV RNA replication and the propagation of infectious virus. CKB is a brain-type creatine kinase isoenzyme and is also detected in a variety of other tissues, including human liver (32). Steady-state levels of CKB in the DRM fraction, as well as in whole-cell lysate of SGR-N cells were compared to those from parental cells by Western blotting. The CKB level in the DRM fraction of replicon cells was higher than that in parental cells (Fig. 1E), confirming the results of the proteome analysis described above. In contrast, the CKB level in whole cells was similar in both cells (Fig. 1E). These results suggest participation of posttranslational modification, such as translocation to the DRM fraction, of CKB in replicon cells.

Figure 2A shows the inhibitory effect on HCV RNA replication of CKB siRNA; siCKB-2, the sequence of which does not overlap with the sequence of siCKB-1 used in the above siRNA screening (Fig. 1D). Transfection with siCKB-2 effectively decreased the cellular level of CKB enzymatic activity (data not shown), as well as the abundance of CKB protein (Fig. 2A), and resulted in 60% reduction in the viral RNA level in SGR-N cells compared to the cells treated with control siRNA. This inhibitory effect of siRNA on HCV RNA abundance was also observed in JFH-1-derived subgenomic replicon (SGR-JFH1) cells. The viral RNA level in the cells transfected with siCKB-2 decreased by 50% compared to the control (Fig. 2A). We also tested the CKB mutant, CKB-C283S, in which Cys at aa 283, near the catalytic site, has been replaced with Ser (Fig. 3A) and which is known to be enzymatically inactive and to work in a dominant-negative manner (22, 29). As expected, overexpression of CKB-C283S resulted in a reduction in HCV RNA replication in SGR-N cells (Fig. 2B). We obtained a similar result in SGR-JFH1 cells, as described below (Fig. 3E).

To further examine the involvement of CKB in HCV RNA replication, we tested the effect of Ccr, a substrate analogue and possible inhibitor for CK in either SGR-N, SGR-JFH1 (Fig. 2C), or Huh7 cells transiently replicating luciferase-subgenomic replicon (data not shown). We found dose-dependent inhibition of HCV RNA replication but no observed effect on total cellular levels of protein and ATP (Fig. 2D) in the replicon setting used.

We next examined whether the knockdown of CKB or treatment with Ccr would abrogate the production of HCVcc. At 72 h posttransfection with siCKB-2, the HCV core level in cells infected with HCVcc was significantly reduced (Fig. 2E). Treatment of the infected cells with Ccr at various concentrations also reduced the intracellular and supernatant core level and subsequently decreased HCVcc production (Fig. 2F). These results demonstrate that suppression of the HCV RNA replication by the siRNA-mediated knockdown of CKB or treatment with CKB inhibitor leads to reduction of the production of infectious virus.

CKB interacts with HCV NS4A. Having established a role for CKB in HCV RNA replication, we then tried to determine to how CKB influences the HCV life cycle. It has been re-